HHS Public Access

Author manuscript

J Mol Cell Cardiol. Author manuscript; available in PMC 2024 August 01.

Published in final edited form as:

J Mol Cell Cardiol. 2023 August ; 181: 33–45. doi:10.1016/j.yjmcc.2023.05.007.

Distinct effects of cardiac mitochondrial calcium uniporter inactivation via EMRE deletion in the short and long term

Hector Chapoy Villanueva[1], **Jae Hwi Sung**[1], **Jackie A. Stevens**[1], **Michael J. Zhang**[1,2], **Peyton M. Nelson**[1], **Saahiti Denduluri**[1], **Feng Feng**[1], **Timothy D. O'Connell**[1], **DeWayne Townsend**[1], **Julia C. Liu, PhD**[1,*]

[1]Department of Integrative Biology and Physiology, University of Minnesota Medical School, Minneapolis, MN 55455, USA

[2]Cardiovascular Division, Department of Medicine, University of Minnesota Medical School, Minneapolis, MN 55455, USA

Abstract

Transport of Ca^{2+} into mitochondria is thought to stimulate the production of ATP, a critical process in the heart's fight or flight response, but excess Ca^{2+} can trigger cell death. The mitochondrial Ca^{2+} uniporter complex is the primary route of Ca^{2+} transport into mitochondria, in which the channel-forming protein MCU and the regulatory protein EMRE are essential for activity. In previous studies, chronic *Mcu* or *Emre* deletion differ from acute cardiac *Mcu* deletion in response to adrenergic stimulation and ischemia/reperfusion (I/R) injury, despite equivalent inactivation of rapid mitochondrial Ca^{2+} uptake. To explore this discrepancy between chronic and acute loss of uniporter activity, we compared short-term and long-term *Emre* deletion using a novel conditional cardiac-specific, tamoxifen-inducible mouse model. After short-term *Emre* deletion (3 weeks post-tamoxifen) in adult mice, cardiac mitochondria were unable to take up Ca^{2+}, had lower basal mitochondrial Ca^{2+} levels, and displayed attenuated Ca^{2+}-induced ATP production and mPTP opening. Moreover, short-term EMRE loss blunted cardiac response to adrenergic stimulation and improved maintenance of cardiac function in an *ex vivo* I/R model. We then tested whether the long-term absence of EMRE (3 months post-tamoxifen) in adulthood would lead to distinct outcomes. After long-term *Emre* deletion, mitochondrial Ca^{2+} handling and function, as well as cardiac response to adrenergic stimulation, were similarly impaired as in short-term deletion. Interestingly, however, protection from I/R injury was lost in the long-term. These data suggest that several months without uniporter function are insufficient to restore bioenergetic response but are sufficient to restore susceptibility to I/R.

Graphical Abstract

[*]Corresponding author: Julia C. Liu, PhD, Address: 2231 6th SE, Minneapolis, MN, 55455, USA, Phone: 612-301-7689, julialiu@umn.edu.

Conflict of Interest: none declared.

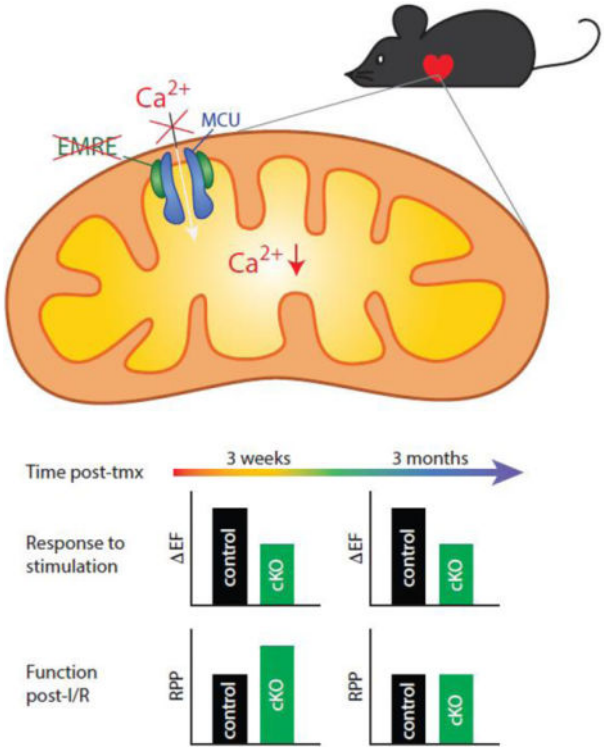

Keywords

mitochondrial calcium uniporter; mitochondria; calcium; permeability transition pore; ATP; ischemia/reperfusion

1. Introduction

The heart, which requires large amounts of energy to continually pump blood, relies primarily on mitochondria to generate ATP [1]. Cardiomyocytes are thus among the most mitochondria-rich cells in the body; approximately 30% or more of the volume of a cardiomyocyte is comprised of mitochondria [2]. Among its many roles in vital cell processes such as gene expression, signal transduction and muscle contraction [3], calcium (Ca^{2+}) has been shown to stimulate mitochondrial ATP production [4]. In the mitochondrial matrix, Ca^{2+} activates pyruvate dehydrogenase (PDH) as well as the tricarboxylic acid (TCA) cycle enzymes alpha-ketoglutarate dehydrogenase and isocitrate dehydrogenase [5,6]. This process is thought to be critical for matching energy supply to demand, such as during periods of increased workload [7]. However, overload of mitochondrial Ca^{2+} can induce opening of the mitochondrial permeability transition pore (mPTP) [8]. Mitochondrial Ca^{2+} overload has been implicated in a range of different pathological disorders [9–12], and Ca^{2+} induced mPTP opening has been linked to cell death in ischemia/reperfusion (I/R) injury in the heart [13,14]. Inhibition of mPTP opening or inhibition of the upstream event of mitochondrial Ca^{2+} uptake could therefore be beneficial therapeutically in myocardial infarction. Deeper understanding of the regulation of mitochondrial Ca^{2+} is thus critical

for targeting mitochondrial dysfunction in pathology while not compromising physiological bioenergetics.

Mitochondrial Ca^{2+} uptake occurs through a highly selective multiprotein Ca^{2+} channel known as mitochondrial Ca^{2+} uniporter complex [15,16] (hereafter referred to as the "uniporter"), located in the inner mitochondrial membrane. The uniporter is made up of multiple auxiliary subunits, including MCU, the transmembrane protein that oligomerizes to form the Ca^{2+}-permeant pore of the complex [17,18] and MCUb, a homologous protein that can act as a negative regulator [19]. Further, the uniporter is regulated by a family of intermembrane space-localized Ca^{2+}-sensing proteins comprising three members, MICU1 [20], MICU2 [21], and MICU3 [22], and by a small transmembrane protein named Essential MCU Regulator (EMRE) [23]. EMRE has been shown to stabilize the uniporter serving as an anchor between MCU and MICU1 [23,24], and in a recently solved structure was shown to bind 1:1 with MCU to allow Ca^{2+} conductance through conformational changes in the tetrameric channel [25].

Recent research has continued to provide insight into the contribution of each subunit in regulating the physiological functions of various organ systems. Multiple mouse models of MCU deletion and inactivation have been used to study the role of mitochondrial Ca^{2+} in the heart. The first mouse model used a gene-trap method to globally delete *Mcu* in the germline in outbred CD-1 mice [26], as germline *Mcu* deletion was embryonic lethal in inbred C57Bl/6 mice. In these $Mcu^{-/-}$ mice, mitochondrial Ca^{2+} uptake was impaired across tissues [27] and intramitochondrial Ca^{2+} was decreased in the heart [28]. As expected, given these findings, sensitivity to Ca^{2+}-induced mPTP opening was decreased; however, germline *Mcu* deletion did not confer protection in an *ex vivo* Langendorff model of I/R injury [26]. This counterintuitive result was supported by similar *ex vivo* I/R data in a study of mouse model expressing cardiac-specific dominant negative *Mcu* [29]. Subsequently, a cardiac-specific tamoxifen-inducible mouse model of *Mcu* deletion (hereafter referred to as Mcu^{cKO} mice) was developed by crossing floxed $Mcu^{fl/fl}$ mice to the αMHC-MerCreMer (*MCM*) transgenic strain, enabling the acute deletion of *Mcu* in adulthood [30,31]. Though intramitochondrial Ca^{2+} levels were unchanged, upon *in vivo* I/R via left coronary artery ligation, infarct area was decreased in adult Mcu^{cKO} mice fed [30] or injected with [31] tamoxifen, showing that acute *Mcu* deletion did protect against I/R injury (see Table 1 in Discussion). Though protection was found in *in vivo* I/R and not found in *ex vivo* I/R, making the type of model used a possible source of this discrepancy, the more likely and interesting possibility would be that mice that have lost MCU acutely have the expected protection against I/R injury, but $Mcu^{-/-}$ and *DN-Mcu* mice that experience chronic loss of uniporter function do not retain protection. While activation of unknown compensatory pathways in the chronic absence of MCU could feasibly explain these findings, whether this could occur over long timescales even in adulthood or requires MCU loss during development is unclear.

In metazoan uniporters, EMRE is essential for the transport of Ca^{2+} through MCU [23]. The first mouse model of CRISPR-mediated deletion of *Emre* in the germline ($Emre^{-/-}$ mice) in outbred mice turned out to have substantial similarity to the $Mcu^{-/-}$ model [32]. The absence of mitochondrial Ca^{2+} uptake, decrease in intramitochondrial Ca^{2+}

concentration, and decrease in sensitivity to Ca^{2+}-induced mPTP opening in mitochondria from *Emre*$^{-/-}$ mice [32] recapitulated findings in *Mcu*$^{-/-}$ mice. Furthermore, like the *Mcu*$^{-/-}$ mice, *Emre*$^{-/-}$ mice did not exhibit protection in the Langendorff *ex vivo* I/R model [32]. Therefore, the potential compensatory response in chronic *Mcu* deletion models occurs as a result of loss of uniporter Ca^{2+} uptake activity and not loss of MCU *per se*. Here we sought to determine how short-term and long-term deletion of *Emre* in the heart would alter mitochondrial and tissue function. We developed a tamoxifeninducible cardiomyocyte-specific model of *Emre* deletion (*Emre*^{cKO} mice) and characterized these mice 3 weeks (short-term) and 3 months (long-term) post-tamoxifen. As expected, we confirmed in the short and long term that EMRE is required for cardiac mitochondrial Ca^{2+} uptake. Like *Emre*$^{-/-}$ mice, *Emre*^{cKO} mice exhibited a significant reduction in cardiac intramitochondrial Ca^{2+} levels and decreased Ca^{2+}-induced mPTP opening, which persisted from short to long-term deletion. Unlike *Emre*$^{-/-}$ mice, however, in *Emre*^{cKO} mice the short-term deletion of *Emre* led to blunted responses to adrenergic stimulation and protection from I/R injury in an *ex vivo* Langendorff model. In the long-term absence of EMRE, mitochondrial Ca^{2+} uptake was still absent in *Emre*^{cKO} cardiac mitochondria, and adrenergic response continued to be attenuated. Strikingly, the protection from I/R injury seen upon short-term EMRE loss was no longer observed with long-term EMRE absence, suggesting that protection from I/R is lost in a time-dependent manner with chronic uniporter inactivity.

2. Methods

2.1. Development of cardiac-specific Emre knockout mouse model (Emre^{cKO})

Emre $^{flox/flox}$ mice (C57BL6/N) from the Mutant Mouse Resource & Research Centers (MMRRC) were crossed with cardiac-specific tamoxifen-inducible Cre mice (αMHC-Mer-Cre-Mer, abbreviated MCM^{+}, C57BL6/J) to generate cardiac-specific *Emre*^{cKO} mice (C57BL6/N and C57BL6/J hybrids). To induce *Emre* deletion, 9- to 11-week-old male and female mice were injected intraperitoneally (i.p.) with tamoxifen (30 mg/kg body weight) per day for 5 days, and experiments were conducted 3 weeks or 3 months post-tamoxifen as described in the text. All groups, including *Emre*$^{flox/flox}$ and *MCM*$^{+}$ controls, received tamoxifen. The animal procedures were approved by the University of Minnesota Institutional Animal Care and Use Committee and performed in compliance with all relevant laws and regulations. Data are shown from female mice and from male mice where indicated.

2.2. Mitochondria heart isolation

Heart mitochondrial fractions were obtained as previously described [32]. Briefly, the heart was isolated and placed in an ice-cold isolation buffer, containing (mM): 225 mannitol, 75 sucrose, 5 MOPS, 0.5 EGTA, 2 taurine, pH 7.2. After being minced and homogenized with a T25 Ultra-Turrax disperser, heart tissue was digested for 5 min using trypsin in cold isolation buffer followed by addition of 0.2% BSA to stop digestion. The homogenates were centrifuged at 500 *g* for 5 min and then the resulting supernatant was centrifuged at 11,000 *g* for 5 min. The final mitochondria pellet was resuspended in isolation buffer and protein concentration was measured by Bradford assay.

2.3. Ca^{2+} retention capacity (CRC), membrane potential ($\Delta\psi$), and swelling

The Ca^{2+} retention capacity (CRC) assay was performed by monitoring extramitochondrial Ca^{2+} levels via the fluorescence of the membrane-impermeable Ca^{2+} indicator Calcium Green-5N (Ca Green-5N, 1.0 μM). Isolated mitochondria were suspended (0.1 mg/mL) in respiration buffer containing (mM): 125 KCl, 2 K_2HPO_4, 20 HEPES, 1 $MgCl_2$, 0.010 EGTA and pH 7.3. The mitochondria were energized with 10 mM succinate and 2 μM of rotenone or where indicated 10 mM glutamate and 5 mM malate. Successive boluses of Ca^{2+} (10 μM) were added to induce mitochondrial Ca^{2+} uptake. Loss of mitochondrial membrane potential ($\Delta\psi$) upon addition of a large bolus of Ca^{2+} (400 μM) was measured via the fluorescence of the indicator safranin (2 μM) [33]. Carbonyl cyanide 4-(trifluoromethoxy)phenylhydrazone (FCCP) was used as uncoupling agent. Mitochondrial swelling was measured in isolated mitochondria upon addition of a large bolus of Ca^{2+} (400 μM) as the reduction of absorbance at 540 nm. Fluorescence or absorbance was monitored using a Synergy H1 microplate reader (BioTek Instruments, Winooski, VT, USA).

2.4. Intramitochondrial Ca^{2+} content ($_mCa^{2+}$)

Intramitochondrial free Ca^{2+} was measured as previously described [32]. Briefly, heart mitochondria were isolated in the isolation buffer supplemented with 2 μM Ru360 and 10 μM CGP-37157 to avoid calcium influx and efflux, respectively, during the isolation process. Isolated mitochondria were loaded with 20 μM of Fluo-4 AM at room temperature and incubated for 45 minutes in the dark. Afterwards, the pellet was washed twice with isolation buffer and then was washed again with isolation buffer without EGTA. Finally, the pellet was resuspended in buffer containing (mM): 137 KCl, 20 HEPES, 2 K_2HPO_4 at pH 7.2. After obtaining the fluorescence of the mitochondrial sample F, to calibrate, F_{max} was obtained after addition of 10 μM of ionomycin and 15 μM of Ca^{2+}, and F_{min} was obtained after addition of 2 mM of EGTA. Fluorescence was monitored using a Synergy H1 microplate reader. Intramitochondrial Ca^{2+} was estimated using the formula: $_mCa^{2+}$ (nM)= K_d*(($F - F_{min}$)/($F_{max} - F$)), where K_d is the dissociation constant for Fluo-4, 335 nM. The data were reported normalized to control groups performed in the same experiment.

2.5. ATP production rate

The ATP production rate was measured in fresh heart mitochondria using the ATP bioluminescence assay Kit CLS II (Roche, 11699695001) [34]. Briefly, 10 μg of protein was added to 75 μL of ATP buffer (mM): 125 KCl, 10 HEPES, 5 $MgCl_2$ and 2 K_2HPO_4, pH: 7.4, along with 75 μL of luciferin/luciferase buffer. Luminescence was monitored using a Synergy H1 microplate reader. The baseline signal was recorded for 1 minute, then 10 mM of succinate or 10 mM glutamate/5 mM malate and 50 μM of ADP were added. The slope was analyzed, and the ATP concentration (nanomoles per minute per mg of protein) was calculated from a fresh ATP standard curve. Where indicated, the ADP buffer was supplemented with 20 μM of Ca^{2+}.

2.6. Immunoblotting

Mitochondrial or cardiac tissue protein was resolved on NuPAGE Bis-Tris 4 to 12% gels (Invitrogen) and transferred to nitrocellulose membranes and incubated with

following antibodies: MCU (1:2000, Cell Signaling, 14997S), EMRE (1:200, Santa Cruz Biotechnology, sc-86337), MICU1 (1:500, Sigma Aldrich, HPA037480), PDH (1:2000, Santa Cruz Biotechnology, sc-377092), p-PDH (Ser293) (1:2000, Cell Signaling, 31866S), CPT1B (1:1000, Proteintech, 22170-1-AP), p-CAMKII (1:1000, Cell Signaling, 12716S), CAMKIIα/β/γ/δ (1:1000, Santa Cruz Biotechnology, sc-5306), CypD (1:1000, abcam, ab110324), GAPDH (1:5000, Cell Signaling, 97166S, VDAC1 (1:1000, Santa Cruz Biotechnology, sc-390996) and then with LI-COR IRDye secondary antibodies. The membranes were scanned on the Licor Odyssey system.

2.7. Blue native PAGE (BN-PAGE)

Freshly isolated cardiac mitochondria were incubated with NativePAGE sample buffer (Invitrogen) containing 2% ReadyShield protease & phosphatase inhibitor cocktail (Sigma) and 2% digitonin [32]. After 20 minutes on ice the samples were centrifuged for 30 minutes at 18,000 *g* at 4 °C. Coomassie blue (5%) was added to the supernatants, then 40 μg of protein was loaded. The electrophoresis running buffers were prepared according to the manufacturer's protocol for the NativePAGE Novex Bis-Tris Gel System (Invitrogen). After electrophoresis gels were transferred onto nitrocellulose membranes for 18 hours at 4 °C. After blocking with 5% milk for 6 hours at 4 °C, membranes were incubated with MCU antibody (1:1000, Sigma Aldrich, HPA016480) overnight at 4 °C and then with HPR-conjugated secondary antibody. The blots were developed with ECL Western Blotting Substrate (Pierce) and quantified using a ChemiDoc MP Imaging System (BioRad).

2.8. Real-Time Quantitative PCR (RT-qPCR)

Heart tissue RNA was isolated by RNA MiniPrep (Zymo Research, R2052). Reverse transcription (10 ng of RNA) and real-time PCR assay were performed by Luna® Universal One-step RT-qPCR kit (New England BioLabs, E3005L) on a Bio-Rad CFX96 System. The following primer sequences were used: MCU, forward primer: 5'-GTGCCCTCTGATGACGTGACGG-3', reverse primer: 5'- ATGACAAGCTTAAAGTCATC-3'; EMRE, forward primer: 5'- CATTTTGCCCAAGCCGGTG-3', reverse primer: 5'-CCTGTGCCCTGTTAATCGTCGT-3'. The following primer sequences were used for reference genes: eukaryotic translation initiation factor EIF35S, forward primer: 5'-CTGAGGATGTGCTGTCTGGGAA-3', reverse primer: 5'-CCTTTGCCTCCACTTCGGTC-3'; ribosomal protein 36B4, forward primer: 5'-GGCCCTGCACTCTCGCTTTC-3', reverse primer: 5'-TGCCAGGACGCGCTTGT-3'[35].

2.9. Oxygen consumption rate (OCR)

As previously described [36], mitochondria were loaded in a 96-well Seahorse plate (4 μg of protein per well) in mitochondrial assay solution (MAS) (mM): 220 mannitol, 70 sucrose, 10 KH_2PO_4, 5 $MgCl_2$, 2 HEPES, 1 EGTA and 0.2% of fatty acid-free BSA, pH: 7.2 supplemented with: 5 mM pyruvate/0.5 mM malate or 40 μM palmitoylcarnitine/0.5 mM malate. Using an Agilent Seahorse XFe96 Analyzer, OCR was analyzed at baseline and following sequential injections of 4mM ADP (state III), 2.5 μg/mL oligomycin (state IV_o), 6 μM FCCP (state III_u), and 4 μM rotenone/4 μM antimycin A. Basal respiration was calculated as the difference between the baseline OCR and post-rotenone/antimycin A

OCR (non-mitochondrial oxygen consumption). The respiratory control ratio (RCR) was calculated as the ratio of state III_u to state IV_o. OCR values were normalized to μg of protein.

2.10. Mitochondrial enzyme activity

As described in [37], Complex I (NADH: ubiquinone oxidoreductase) activity was measured by following the absorbance change of NADH at 340 nm (ε: 6.2 mM^{-1} cm^{-1}) using potassium phosphate buffer (50 mM potassium phosphate dibasic with 50 mM of potassium phosphate monobasic, pH: 7.5), 0.100 mM NADH, 3 mg/mL BSA, 0.300 mM KCN and 0.060 mM ubiquinone. Rotenone (10μM) was added to inhibit Complex I to allow subtraction of inhibitor-insensitive activity from the data. Complex II (succinate dehydrogenase) activity was measured spectrophotometrically at 600 nm (ε: 19.1 mM^{-1} cm^{-1}) in potassium phosphate buffer (25 mM potassium phosphate dibasic with 25 mM potassium phosphate monobasic, pH: 7.5), 20 mM succinate, 0.080 mM 2,6-dichlorophenolindophenol (DCPIP), 1 mg/mL BSA, 0.300 mM KCN and 0.050 mM decylubiquinone (DUB). Malonate (10 mM) was added to inhibit complex II. Complex I and II activity were normalized to citrate synthase activity (CS), measured at 412 nm (ε : 13.6 mM^{-1} cm^{-1}) in Tris 100 mM (pH: 8.0) buffer containing 0.1% Triton X-100, 0.100 mM 5,5'-dithiobis(2-nitrobenzoic acid) (DTNB), 0.300 mM acetyl CoA, and 0.5 mM oxaloacetic acid. All assays were performed in triplicate on a Synergy H1 microplate reader at 37 °C in volumes of 200 μl/ well at a protein concentration of 0.05 mg/ml. The enzymatic activities were calculated as: nmol min^{-1} mg^{-1} = (Δ Absorbance/min × 1,000)/[(extinction coefficient × volume of sample) × (sample protein concentration)].

2.11. H_2O_2 production

Mitochondrial ROS generation was measured spectrofluorometrically (560 nm excitation and 590 nm emission) on a Synergy H1 microplate reader with the H_2O_2-sensitive dye Amplex Red (50 μM) (Invitrogen, A1222) and horseradish peroxidase (5 U/mL). Mitochondria (100 μg protein) were incubated in a solution containing (in mM): 120 KCl, 10 Tris-HCl, 5 MOPS, 5 K_2HPO_4 and 10 μM EGTA, pH 7.4. Baseline fluorescence was monitored for 1 minute, then 10 mM glutamate/5 mM malate was added and monitoring continued for 6 or more minutes. After subtraction of values from a blank well containing no mitochondria, slopes were calculated for the first 5 minutes after addition of glutamate/malate, and converted to units of pmol H_2O_2/(min*mg protein) using a linear fit to a standard curve of Amplex Red fluorescence across H_2O_2 concentrations. As positive and negative controls, antimycin A (500 nM) or 2,4-dinitrophenol (10 nM) respectively were present with a mitochondria sample in separate wells.

2.12. Protein carbonylation assay

The levels of protein carbonyl groups were assessed using the protein carbonyl assay kit (Abcam) according to manufacturer's instructions. Briefly, freshly isolated mitochondria (100 μg) were diluted with 12% SDS and incubated with DNPH solution for 15 minutes at room temperature, then the reaction was neutralized. Gel electrophoresis (3 μg of protein per sample) and immunoblotting was performed as described under immunoblotting above with the anti-DNP antibody provided in the kit.

2.13. Transthoracic echocardiography

To measure left ventricular (LV) response to beta-adrenergic stimulation, we used serial transthoracic echocardiography to evaluate LV ejection fraction as a surrogate for LV function. We used a Vevo 2100 (Fujifilm VisualSonics, Toronto, CA) ultrasound imaging system to perform echocardiography. Mice were anesthetized with 2% isoflurane and affixed in a supine position to an ECG measuring platform heated to 37C. Ultrasound measurements were performed with a MS400 linear array ultrasound probe operating between 22–55 MHz. The ultrasound probe was placed across the mouse's thorax to obtain a parasternal long axis view of the heart, and to capture two-dimensional and M-mode cine at mid-LV level. After acquisition of baseline images, at a heart rate between 400 and 550 bpm, mice were injected with isoproterenol (0.4 μg/kg) and serial images were taken every minute for five minutes. Echocardiography images were then analyzed using the Vevo Lab software. LV ejection fraction was calculated using the modified Quinones method from M-mode measurements of at least 3 different cardiac cycles from the parasternal long axis view.

2.14. Langendorff ex vivo ischemia/reperfusion (I/R)

The mice were euthanized using 100U of heparin and 250 mg/kg of sodium pentobarbital. The hearts were then harvested and perfused on the Langendorff apparatus using modified Krebs buffer (in mM): 118 NaCl, 0.5 EDTA, 4.7 KCl, 1.2 $MgSO_4$, 1.2 Na_2HPO_4, 15 glucose, 2.5 $CaCl_2$, 25 $NaHCO_3$, and 0.5 pyruvate. Oxygen probes (Microelectrodes, Inc.) were used throughout the protocol to monitor oxygen, sampling both the cardiac effluent and perfusate. The left ventricular pressure was measured using a balloon filled with water that was coupled to a solid-state pressure transducer (Millar Instruments). After 20 minutes of equilibration on the apparatus, the hearts were subjected to 20 minutes of no-flow global ischemia, followed by 90 minutes of reperfusion. Coronary flow was monitored by an ultrasonic flow probe (Transonic). At baseline the cannula oxygen levels were 524 ± 18 mmHg, while during hypoxia they were 175 ± 11 mmHg. At the start of reperfusion, effluent samples were collected to measure creatine kinase (CK) release, an indicator of heart damage. Heart rate and left ventricular developed pressure were also recorded to calculate the rate pressure product (RPP = HR × DP).

2.15. Data analysis

Data are expressed as mean ± standard deviation (SD). Unpaired Student's t-test, one-way ANOVA or two-way ANOVA were performed when appropriate to compare experimental groups. A difference was considered statistically significant when $p<0.05$. Data processing and statistical tests were carried out with GraphPad Prism (v.9.3.1, San Diego, CA, USA).

3. Results

3.1. Emre deletion eliminates mitochondrial Ca^{2+} uptake

Emre$^{flox/flox}$ (*Emre*$^{fl/fl}$) mice were crossed with the well-characterized αMHC-MerCreMer (*MCM*$^{+}$) transgenic mouse line to generate a model of acute tamoxifen-inducible cardiomyocyte-specific *Emre* deletion in adulthood. We confirmed that 3 weeks post-tamoxifen injection, *Emre* mRNA expression decreased by 92.5% (Fig. S1A) and protein

expression was reduced by 90% in *Emre*^{cKO} mitochondria relative to *MCM*$^{+}$ and *Emre*$^{fl/fl}$ controls (Fig. 1A). MCU protein expression also decreased but to a lesser extent (60% reduction), but no decrease was observed in *Mcu* mRNA expression (Fig. S1B), suggesting that in the absence of EMRE downregulation of MCU occurs not at the transcriptional level but potentially due to diminished protein stability. No differences were observed in the levels of other uniporter proteins, for instance MICU1 (Fig. 1A and Fig. S1C), nor proteins involved in mitochondrial Ca^{2+} efflux, including the $Na^{+}/Ca^{2+}/Li^{+}$ exchanger (NCLX) and Leucine zipper EF-hand transmembrane protein 1 (Letm1) (Fig. S1D). Blue native polyacrylamide gel electrophoresis (BN-PAGE) analysis of cardiac mitochondria revealed that loss of EMRE decreased the molecular weight of the uniporter complex from over 440 kDa [23,38] to approximately 300 kDa, as reported previously [32]. To assess how Ca^{2+} handling is affected by EMRE deletion, we performed Ca^{2+} retention capacity (CRC), mitochondrial swelling, and membrane potential assays. *Emre*^{cKO} cardiac mitochondria were unable to take up Ca^{2+} in CRC assays, unlike control *MCM*$^{+}$ and *Emre*$^{fl/fl}$ mitochondria, in which normal mitochondrial Ca^{2+} uptake was observed (Fig. 1C–D, S1E–F). To determine whether *Emre*^{cKO} mitochondria can undergo mitochondrial Ca^{2+} overload-induced mitochondrial permeability transition pore (mPTP) opening, we analyzed mitochondrial swelling after adding a large Ca^{2+} bolus. *Emre*^{cKO} mitochondria were resistant to swelling relative to *MCM*$^{+}$ and *Emre*$^{fl/fl}$ controls (Fig. 1E, S1G), presumably due to loss of mitochondrial Ca^{2+} uptake. Similarly, in an assay using the dye safranin to monitor depolarization of mitochondrial membrane potential, *Emre*^{cKO} mitochondria were able to maintain mitochondrial membrane potential after addition of a large Ca^{2+} bolus, in contrast to *MCM*$^{+}$ and *Emre*$^{fl/fl}$ controls (Fig. 1F).

3.2. Emre deletion leads to lower intramitochondrial Ca^{2+} content and attenuated Ca^{2+}-stimulated ATP production

Once we confirmed that cardiac-specific EMRE deletion eliminated mitochondrial Ca^{2+} uptake in heart mitochondria as expected, our next question was whether this deletion affects basal intramitochondrial Ca^{2+} ($_{m}Ca^{2+}$) levels. Relative to *MCM*$^{+}$ and *Emre*$^{fl/fl}$ controls, *Emre*^{cKO} mitochondria had lower $_{m}Ca^{2+}$ levels, as might be expected in the absence of mitochondrial Ca^{2+} uptake activity (Fig. 2A). As the dephosphorylation of PDH is $_{m}Ca^{2+}$-dependent [5], we next measured the ratio of phosphorylated pyruvate dehydrogenase (p-PDH) to total PDH in *Emre*^{cKO} heart mitochondria and found a ~20% increase compared with control mitochondria (Fig. 2B). These data support that loss of EMRE leads to decreased $_{m}Ca^{2+}$ levels. Because $_{m}Ca^{2+}$ has been shown to activate mitochondrial energy production [39], we sought to assess whether mitochondrial respiration is affected by *Emre* deletion. Seahorse analysis of isolated mitochondria supplied with either pyruvate and malate or palmitoylcarnitine and malate did not reveal significant differences in oxygen consumption rate (OCR) at baseline, after ADP addition, or after FCCP treatment to decouple mitochondria and promote maximal respiration (Fig. S2A–B). Respiratory control ratios (RCR) likewise were similar between control and *Emre*^{cKO} heart mitochondria for either substrate combination (Fig. S2C–D). These data suggest that, unlike *Mcu* deletion in heart and skeletal muscle [40–42], short-term *Emre* deletion did not lead to a shift toward for fatty acid oxidation in cardiac mitochondria. Consistently, protein levels of carnitine O-palmitoyl transferase 1b (CPT1) were similar across genotypes (Fig. S2E). Furthermore,

though dysfunction of Complex I of the mitochondrial electron transport chain has been associated with increased uniporter stability [43,44], we did not find significant differences in the activity of either respiratory Complex I or Complex II in short-term *Emre*^{cKO} and control heart mitochondria (Fig. S2F–G). We then asked whether directly measuring ATP production rate in the presence and absence of Ca^{2+} would reveal Ca^{2+}-induced energetic differences in *Emre*^{cKO} and control cardiac mitochondria. While the rate of ATP production upon providing ADP was similar in all groups, the addition of Ca^{2+} induced an increase in ATP production rate in control mitochondria but not in *Emre*^{cKO} mitochondria (Fig. 2C, S2H). These results suggest that the loss of EMRE prevents stimulation of ATP production by mitochondrial Ca^{2+} uptake.

3.3. Short-term Emre deletion leads to reduced response to β-adrenergic stimulation

We next sought to determine whether cardiac-specific *Emre* deletion in adult mice had physiological consequences in the short term. At 3 weeks post-tamoxifen, *Emre*^{cKO} mice showed no overt phenotype and had similar body weights and heart weights as controls (Fig. S3A–B). Because the Ca^{2+}-stimulated rate of ATP production was reduced in *Emre*^{cKO} cardiac mitochondria, we reasoned that loss of EMRE might attenuate an increase in cardiac energy production upon increased workload. We thus evaluated the ability of *Emre*^{cKO} mice to respond to β-adrenergic stimulation. Using echocardiography, we measured left ventricular ejection fraction (EF) and fractional shortening (FS) at baseline and then each minute up to 5 minutes after intraperitoneal injection of the β-adrenergic receptor agonist isoproterenol. In *MCM*$^{+}$ and *Emre*$^{fl/fl}$ mice, EF (Fig. 3A) and FS (Fig. 3B) increased substantially upon stimulation, but in *Emre*^{cKO} mice this response was more gradual. Although interplay between CaMKII and MCU in the context of adrenergic stimulation has been documented [45,46], we did not observe a difference in the phosphorylation status of CaMKII with *Emre* deletion (Fig. S3C). These results suggest that the absence of rapid mitochondrial Ca^{2+} uptake impairs the heart's ability to respond to adrenergic stimulation, in agreement with previous studies investigating acute cardiac deletion of *Mcu*.

3.4. Short-term Emre deletion preserves cardiac function in I/R

So far, we have shown that the short-term deletion of *Emre* in the adult mouse heart is sufficient to block Ca^{2+} uptake into mitochondria and decrease $_{m}Ca^{2+}$ levels. Consistent with these effects, *Emre*^{cKO} mitochondria are resistant to mPTP opening following $_{m}Ca^{2+}$ overload. Cell death due to mPTP opening is thought to contribute to I/R injury; therefore, we evaluated whether *Emre*^{cKO} mice would show preserved cardiac function in an *ex vivo* Langendorff perfusion model of I/R injury. Our results show that during reperfusion *Emre*^{cKO} hearts maintained higher rate pressure product (RPP) relative to baseline pre-ischemic levels compared with control hearts, and this protection is even preserved until the end of the reperfusion period (Fig. 4A). Likewise, measures of systolic and diastolic pressure changes (dP/dt_{max} and dP/dt_{min}, respectively) were preserved to a greater degree during reperfusion in *Emre*^{cKO} mice compared to control mice (Fig. 4B–C). To determine the degree of injury in the hearts, we measured the release of creatine kinase (CK), a marker of cardiomyocyte membrane injury, and found reduced CK release in *Emre*^{cKO} mice relative to controls (Fig. 4D). Although Cyclophilin D (CypD) is a known activator of the mPTP, resistance to pore opening does not appear to be mediated by any decrease in CypD protein

expression (Fig. S3D). Altogether, the data show that shortly after the loss of EMRE in adulthood, hearts are protected against I/R injury, consistent with the idea that preventing mitochondrial Ca^{2+} uptake during I/R prevents tissue damage.

3.5. Mitochondrial Ca^{2+} handling remains impaired in $Emre^{cKO}$ mice over time

Thus far, we have confirmed that the short-term loss of EMRE in adulthood is consistent with many aspects of the Mcu^{cKO} phenotype, further solidifying that like MCU, EMRE is essential for uniporter activity. We next sought to explore why germline $Mcu^{-/-}$ and $Emre^{-/-}$ mice do not exhibit the impaired response to adrenergic stimulation and protection from I/R injury seen in the Mcu^{cKO} mice. This discrepancy has been attributed to remodeling in the chronic absence of uniporter activity, but whether long timescales alone are sufficient for remodeling is unclear. Therefore, we waited 3 months post-tamoxifen, which we will refer to as long-term *Emre* deletion, to reexamine the phenotype of $Emre^{cKO}$ mice. We first measured the mRNA and protein expression of EMRE and MCU in isolated cardiac mitochondria to confirm that protein levels relative to controls remained significantly decreased (Fig. 5A), although as before *Mcu* mRNA is expressed at control levels (Fig. S4A–B). Expression of MICU1 as well as the efflux proteins NCLX and LETM1 were still unchanged between $Emre^{cKO}$ and control mitochondria (Fig. 5A, S4C–D). Similarly, we verified that at 3 months post-tamoxifen the molecular weights of the uniporter complex with and without EMRE remained the same as at 3 weeks post-tamoxifen (Fig. 5B). Next, we conducted CRC, swelling, and membrane potential assays in $Emre^{cKO}$ mitochondria 3 months post-tamoxifen and found that the loss of mitochondrial Ca^{2+} uptake and resistance to mPTP opening were maintained, as observed in short-term deletion (Fig. 5C–F, S4E–G).

Similarly, measurements of free $_{m}Ca^{2+}$ levels in $Emre^{cKO}$ mitochondria 3 months post-tamoxifen suggested that $_{m}Ca^{2+}$ remained decreased (Fig. 6A), consistent with significantly elevated p-PDH to total PDH ratio in $Emre^{cKO}$ mitochondria (Fig. 6B). As found in the short-term, long-term *Emre* deletion did not alter OCR or RCR in either pyruvate/malate or palmitoylcarnitine/malate substrate conditions (Fig. S5A–D). Hence, long-term absence of *Emre* deletion did not appear to lead to a shift toward preferential fatty acid oxidation, and correspondingly CPT1 protein levels were unchanged (Fig. S5E). Complex II activity remained similar between groups 3 months post-tamoxifen; Complex I activity in $Emre^{cKO}$ mitochondria exhibited a slight downward trend that however did not reach significance ($p = 0.0735$) (Fig. S5F–G). Additionally, though baseline ATP production rates were similar in $Emre^{cKO}$ and control mitochondria, the increase in ATP production rate in the presence of Ca^{2+} was still absent in $Emre^{cKO}$ mitochondria (Fig. 6C, S5H). Taken together, these data suggest that, at the level of isolated mitochondria, long-term absence of EMRE does not lead to substantially different effects compared to those of the short-term.

3.6. β-adrenergic response remains diminished in long-term Emre deletion, but protection against I/R injury is lost

After confirming that long-term *Emre* deletion revealed similar mitochondrial Ca^{2+} handling as in short-term *Emre* deletion, we sought to assess at 3 months post-tamoxifen how $Emre^{cKO}$ mice responded to β-adrenergic stimulation. We first verified that long-term *Emre* deletion did not lead to any significant changes in body weight or heart weight (Fig.

S6A–B). We then repeated the echocardiography experiment measuring ejection fraction and fractional shortening at baseline and after isoproterenol injection. Notably, in contrast to germline *Emre* or *Mcu* deletion, long-term cardiac-specific *Emre* deletion in adulthood still resulted in diminished adrenergic response (Fig. 7A–B). The phosphorylation status of CaMKII also remained similar between groups (Fig. S6C). This result suggests that the fight or flight response cannot be restored in a time-dependent manner in the chronic absence of rapid mitochondrial Ca^{2+} uptake ability. After confirming that β-adrenergic response remained blunted in mice with long-term cardiac *Emre* deletion, we next sought to determine whether protection from I/R injury is similarly preserved. We repeated the Langendorff *ex vivo* I/R experiment in 3-month post-tamoxifen $Emre^{cKO}$ and control hearts. Surprisingly, and in contrast to short-term *Emre* deletion, we observed that long-term *Emre* deletion did not have a significant effect relative to controls on RPP, dP/dt_{max}, dP/dt_{min}, or CK release following reperfusion (Fig. 7C–F). This lack of protection in long-term *Emre* deletion could not be attributed to increased CypD expression, as CypD protein levels did not vary significantly between $Emre^{cKO}$ and control mitochondria (Fig. S6D).

We then considered that apart from excessive mitochondrial Ca^{2+}, reactive oxygen species (ROS) can also act as a trigger for mPTP opening [47]. Despite equivalent rates of ROS production in isolated $Emre^{cKO}$ and control mitochondria in the short and long term as measured by Amplex Red (Fig. S7A–C), assessment of protein carbonylation revealed that $Emre^{cKO}$ mitochondria have significantly less oxidative stress in the short-term than in the long-term (Fig. 8A–B). Furthermore, although oxidative stress levels between $Emre^{cKO}$ and control mitochondria in the long-term are similar, in the short-term $Emre^{cKO}$ mitochondria show a trend toward decreased oxidative stress relative to control mitochondria that approaches significance ($p = 0.0548$). These data suggest that a transient decline in oxidative stress in short-term but not long-term *Emre* deletion is associated with protection against I/R injury; over time, oxidative stress returns to control levels, and concurrently protection against I/R injury conferred by acute loss of mitochondrial Ca^{2+} uniporter activity is lost.

4. Discussion

Here we present the novel finding that cardiac-specific *Emre* deletion in adult mice has distinct effects in the short and long term. While a blunted response to isoproterenol is preserved from 3 weeks to 3 months after *Emre* deletion, an initial protection against I/R injury is no longer observed after 3 months. This dichotomy exists despite our data showing that in isolated mitochondria at both time points *Emre* deletion eliminates mitochondrial Ca^{2+} uptake and reduces sensitivity to Ca^{2+}-induced mPTP opening.

Lack of rapid mitochondrial Ca^{2+} uptake was also seen in mitochondria from mice with germline *Mcu* or *Emre* deletion as well as mice undergoing cardiac-specific *Mcu* deletion in adulthood [30,31]. Our results in a new cardiac-specific *Emre* knockout mouse model support the multiple studies showing that EMRE is essential to uniporter function [23,24,32]. Furthermore, like $Mcu^{-/-}$ and $Emre^{-/-}$ mice [28,32] but unlike Mcu^{cKO} mice [30,31], $Emre^{cKO}$ mice have reduced cardiac intramitochondrial Ca^{2+} concentration, with lasting effects even 3 months after tamoxifeninduced deletion. In $Emre^{cKO}$ mice, we also observe a large decrease in MCU expression, to a greater extent than observed in the

germline *Emre*$^{-/-}$ mice in which MCU decreased only slightly [32]. Our findings in these mice are thus not attributable solely to the absence of EMRE alone; rather, *Emre*^{cKO} mice represent another model in which the uniporter is nonfunctional. Nonetheless, in both *Emre*^{cKO} and germline *Emre*$^{-/-}$ mice, and in the germline *Mcu*$^{-/-}$ mice where EMRE was significantly decreased [28], the data suggest that a coordinated downregulation of MCU in the absence of EMRE and vice versa leads to lower intramitochondrial Ca^{2+} levels. As EMRE expression was not reported in *Mcu*^{cKO} mice, it is possible that lesser EMRE downregulation with MCU in these circumstances might explain why intramitochondrial Ca^{2+} was unchanged in *Mcu*^{cKO} mice [30,31].

Despite reduced basal intramitochondrial Ca^{2+} levels after short-term *Emre* deletion, *Emre*^{cKO} cardiac mitochondria produced ATP at the same rate as control mitochondria when supplied with ADP without Ca^{2+}. This result echoes previous measurements of oxygen consumption or ATP production in *Mcu*$^{-/-}$, *Emre*$^{-/-}$, or *Mcu*^{cKO} cardiac mitochondria [28,30,32]. However, Ca^{2+}-induced stimulation of ATP production was observed in control but not *Emre*^{cKO} and other uniporter-deficient cardiac mitochondria [28,30], consistent with the uniporter's purported role in delivering Ca^{2+} to the matrix to provide a boost in ATP. Thus, in the absence of a functional uniporter, matching of energy supply to demand, for instance in the fight or flight response, might be expected to be attenuated. Consistent with this hypothesis, here we show with echocardiography that short-term deletion of *Emre* in adulthood, as was shown for *Mcu* deletion in *in vivo* hemodynamics experiments [30,31], resulted in impaired cardiac contractile response to adrenergic stimulation (see Table 1). In contrast, the hearts of global *Mcu*$^{-/-}$ and *Emre*$^{-/-}$ mice responded indistinguishably from wild-type mice to isoproterenol, measured in the former by cardiac catheterization [28] and in the latter by echocardiography [32]. Recent work has shown that Langendorff-perfused global *Mcu*$^{-/-}$ hearts show no increase in mitochondrial Ca^{2+} following isoproterenol addition, yet contractility increases similarly in *Mcu*$^{-/-}$ and wild-type hearts [48]. These results suggest that in the *Mcu*$^{-/-}$ and *Emre*$^{-/-}$ models, the chronic absence of uniporter activity beginning in the germline may have led to compensatory mechanisms that act to meet increased energy demand. However, what form this compensation takes or when it occurs are unclear. To address the latter question, we assessed *Emre*^{cKO} mice at a long time interval (3 months) after tamoxifen administration in adulthood and found that impaired adrenergic response persisted even after long-term EMRE deletion. Although it cannot be excluded that recovery of the rapid response to adrenergic stimulation could gradually take place at timescales longer than 3 months after the loss of uniporter activity starting in adulthood, one possibility is that restoration of the adrenergic response in global *Mcu*$^{-/-}$ and *Emre*$^{-/-}$ mice does not occur merely in a time-dependent manner and instead may require the absence of uniporter function during embryogenesis. Notably, the expression of *DN-Mcu* driven by the αMHC promoter, which is expressed in the myocardium shortly after birth [49], also results in reduced response to isoproterenol [29]. Taken together, one might speculate that the onset of uniporter deficiency at any time *after* birth stably attenuates the ability of the mitochondria to respond to a sudden increase in energy demand in the fight or flight response. It remains to be tested whether compensation for uniporter loss in adulthood can occur gradually over timescales longer than 3 months or whether compensation is only

possible when uniporter loss is experienced early in development in conditions of germline *Mcu* or *Emre* deletion.

The inactivation of mitochondrial Ca^{2+} uptake due to *Emre* deletion would be predicted to protect against I/R injury, and in line with this reasoning, at 3 weeks post-tamoxifen, $Emre^{cKO}$ mice were able to better maintain cardiac function compared with controls in an *ex vivo* Langendorff I/R model. These results are consistent with studies in Mcu^{cKO} mice undergoing *in vivo* I/R [30,31], demonstrating that protection from I/R can manifest in both *in vivo* and *ex vivo* models (see Table 1). Hence, this experimental distinction is not the cause of divergent results in Mcu^{cKO} mice (shown *in vivo* to be protected from I/R) compared with $Mcu^{-/-}$, $Emre^{-/-}$, and *DN-Mcu* mice (shown *ex vivo* to be unprotected). Moreover, it was previously unclear whether the lack of protection against I/R injury in $Mcu^{-/-}$, $Emre^{-/-}$, and *DN-Mcu* mice arose from compensatory cellular pathways in response to chronic uniporter loss, and if so whether these pathways are only active when the uniporter is absent in development or are activated as function of time. Our data support the latter hypothesis, as by 3 months post-tamoxifen, $Emre^{cKO}$ hearts exhibited a similar decrease in cardiac function during I/R as control hearts, suggesting that the protection from I/R injury evident at 3 weeks post-tamoxifen was lost in the intervening time. We conclude that although mice gain protection from I/R injury after acute deletion of *Mcu* or *Emre* in adulthood, this effect appears to be transient. Within a few months, $Emre^{cKO}$ hearts, from which isolated mitochondria are still unable to rapidly take up Ca^{2+}, experience I/R-induced damage to roughly the same extent as control hearts. Furthermore, concurrently with I/R protection in short-term *Emre* deletion, protein carbonylation potentially decreases but later recovers to control levels in the long term. This interesting phenomenon argues that time-dependent compensation for uniporter loss, potentially due to a return to baseline oxidative stress levels, is sufficient to restore susceptibility to I/R, but the nature of this compensation remains incompletely resolved.

We examined multiple cellular pathways known to be linked to MCU activity to determine whether or not in the short- or long-term absence of EMRE these pathways would be altered. Loss of MCU has been shown to alter metabolic substrate preference in the heart and skeletal muscle, in which glucose oxidation is impaired or unchanged while fatty acid oxidation is favored [40–42]. Our data suggest that OCR in the presence of substrates for either glucose oxidation or fatty acid oxidation is similar between control and $Emre^{cKO}$ heart mitochondria in both the short-and long-term. However, it was noted within one study that although OCR measured in Langendorff-perfused and paced hearts increased in *DN-Mcu* mice, Seahorse analysis of control and *DN-Mcu* isolated mitochondria showed no differences [29]. Hence, though we were unable to detect intrinsic mitochondrial differences, further study is needed to uncover metabolic alterations, including potentially fuel preference, in animals with short- and long-term *Emre* deletion.

Additionally, it has been shown that during chronic β-adrenergic stimulation, CaMKIIδB activation upregulates *Mcu* expression at the transcriptional level [45]. However, in the context of both short- and long-term EMRE loss our data show that while MCU protein decreases, CaMKII phosphorylation as well as *Mcu* mRNA levels remain unchanged. Indeed, the modulation of uniporter activity was shown to be downstream of the CaMKII

pathway, and not necessarily vice versa. Similarly, decreased Complex I activity in multiple contexts was shown to lead to compensatory increase in MCU levels and activity [43,44]; whether alterations in MCU activity can reciprocally impact Complex I is less clear. Mild decreases in Complex I and II protein levels were previously observed following acute isoproterenol challenge in *Mcu*^{cKO} hearts 3 months post-tamoxifen [40]. In our study, though no statistically significant decrease in Complex II activity occurred in short- or long-term *Emre* deletion, and short-term *Emre*^{cKO} and control Complex I activity were also similar, at the long-term timepoint Complex I activity trended downwards in *Emre*^{cKO} mitochondria relative to controls, nearly achieving significance. Since it is thought that Complex I and MCU interact such that mild ROS leak from Complex I oxidizes MCU [44], one might speculate that gradually over time, a prolonged absence of this interaction in *Emre*^{cKO} mice could result in even slightly increased oxidative damage to Complex I itself that may decrease its activity. The interaction of Complex I and the uniporter complex, and how perturbation thereof might directly and indirectly affect sensitivity to I/R injury, is amply deserving of future study.

Furthermore, we observed that protein carbonylation is transiently decreased in the short-term absence of EMRE relative to long-term EMRE absence. These data, which temporally correlate with the transient protection from I/R injury, are notable given the well-documented involvement of ROS in opening the mPTP [47]. A gradual decline in Complex I activity and potential uptick in ROS leakage may play a part in the resurgence of oxidative stress in the long-term absence of EMRE, yet what mediates the transient decrease in oxidative damage is still an open question. Which proteins undergo less or more oxidation in the short or long term is also important: for instance, oxidation of CypD is reported to target it to the mitochondrial inner membrane where it can activate mPTP [50]. The germline loss of MCU has been suggested to lead to alterations in the post-translational modification status of CypD that prime mitochondria toward mPTP opening [51]. More detailed study in *Emre*^{cKO} mice of time-dependent CypD expression and modifications, particularly oxidation, is warranted. Finally, cardiomyocytes that chronically lack a functional uniporter may undergo a cell death pathway in I/R distinct from mPTP-triggered necroptosis, given evidence that the CypD inhibitor Cyclosporine A is protective in I/R in wild-type hearts but not *Mcu*$^{-/-}$ or *Emre*$^{-/-}$ hearts [26,32]. What this cell death pathway or pathways might be or what might lead to its activation during the chronic absence of uniporter activity is still unclear.

In summary, we have reported the characterization of a novel tamoxifen-inducible cardiac-specific mouse model of *Emre* deletion, with which we have examined mitochondrial Ca^{2+} handling, response to adrenergic stimulation, and susceptibility to I/R injury at short (3 week) and long (3 month) post-tamoxifen time points. In most respects long-term *Emre* deletion closely resembled short-term *Emre* deletion. In isolated mitochondria, the differences between *Emre*^{cKO} and controls at 3 weeks post-tamoxifen – lack of mitochondrial Ca^{2+} uptake, increased p-PDH to total PDH ratio, reduced Ca^{2+} levels, resistance to Ca^{2+}-induced swelling, and attenuated Ca^{2+}-stimulated ATP production – were still present at 3 months post-tamoxifen. We found that *Emre* deletion in both the short- and long-term impaired isoproterenol-induced increase in contractility; however, only short-term *Emre* deletion was protective against reduced cardiac function during I/R, potentially due to

reduced oxidative stress that appears restricted to the short-term time point. This discrepancy underscores that the compensatory mechanism that allows only mice lacking a functional uniporter starting in the germline to retain their adrenergic response is fundamentally different from the mechanism that in the span of a few months following uniporter loss in adult mice restores sensitivity to I/R. The nature of these uniporter deficiency-induced pathways and the cellular changes they elicit remain a complex problem to be addressed in future research.

Supplementary Material

Refer to Web version on PubMed Central for supplementary material.

Funding

This work was supported by the National Institutes of Health [1K22HL137901 and 1R01HL164491 to J.C.L].

Acknowledgements

We are grateful to Dr. Elizabeth Murphy and members of the Liu and Murphy labs for thoughtful discussions and feedback. We thank Lynn Hartweck and Dr. Madjda Bellamri for their help in optimizing methods to measure respiratory complex activity. We would also like to thank Maximiliano and Dorotea for their everlasting support.

References

[1]. Doenst T, Nguyen TD, Abel ED, Cardiac metabolism in heart failure: implications beyond ATP production, Circ Res. 113 (2013) 709–724. 10.1161/CIRCRESAHA.113.300376. [PubMed: 23989714]

[2]. Barth E, Stämmler G, Speiser B, Schaper J, Ultrastructural quantitation of mitochondria and myofilaments in cardiac muscle from 10 different animal species including man, J. Mol. Cell. Cardiol 24 (1992) 669–681. 10.1016/0022-2828(92)93381-s. [PubMed: 1404407]

[3]. Duchen MR, Verkhratsky A, Muallem S, Mitochondria and calcium in health and disease, Cell Calcium. 44 (2008) 1–5. 10.1016/j.ceca.2008.02.001. [PubMed: 18378306]

[4]. Glancy B, Balaban RS, Role of mitochondrial Ca2+ in the regulation of cellular energetics, Biochemistry. 51 (2012) 2959–2973. 10.1021/bi2018909. [PubMed: 22443365]

[5]. Denton RM, Randle PJ, Martin BR, Stimulation by calcium ions of pyruvate dehydrogenase phosphate phosphatase, Biochem J 128 (1972) 161–163. 10.1042/bj1280161. [PubMed: 4343661]

[6]. Denton RM, McCormack JG, The role of calcium in the regulation of mitochondrial metabolism, Biochem. Soc. Trans 8 (1980) 266–268. [PubMed: 7399049]

[7]. Kwong JQ, The mitochondrial calcium uniporter in the heart: energetics and beyond, J Physiol. 595 (2017) 3743–3751. 10.1113/JP273059. [PubMed: 27991671]

[8]. Kwong JQ, Molkentin JD, Physiological and Pathological Roles of the Mitochondrial Permeability Transition Pore in the Heart, Cell Metabolism. 21 (2015) 206–214. 10.1016/j.cmet.2014.12.001. [PubMed: 25651175]

[9]. Santulli G, Xie W, Reiken SR, Marks AR, Mitochondrial calcium overload is a key determinant in heart failure, Proc. Natl. Acad. Sci. U.S.A 112 (2015) 11389–11394. 10.1073/pnas.1513047112. [PubMed: 26217001]

[10]. Vallejo-Illarramendi A, Toral-Ojeda I, Aldanondo G, López de Munain A, Dysregulation of calcium homeostasis in muscular dystrophies, Expert Rev Mol Med. 16 (2014) e16. 10.1017/erm.2014.17. [PubMed: 25293420]

[11]. and P.P. Giampaolo Morciano, Massimo Bonora, Gianluca Campo, Giorgio Aquila, Paola Rizzo, Carlotta Giorgi, Mariusz R. Wieckowski, Mitochondrial Dynamics in Cardiovascular Medicine, 2017. 10.1007/978-3-319-55330-6_9.

[12]. Martin SD, McGee SL, The role of mitochondria in the aetiology of insulin resistance and type 2 diabetes, Biochim Biophys Acta. 1840 (2014) 1303–1312. 10.1016/j.bbagen.2013.09.019. [PubMed: 24060748]

[13]. García-Rivas GDJ, Carvajal K, Correa F, Zazueta C, Ru360, a specific mitochondrial calcium uptake inhibitor, improves cardiac post-ischaemic functional recovery in rats in vivo., British Journal of Pharmacology. 149 (2006) 829–837. 10.1038/sj.bjp.0706932. [PubMed: 17031386]

[14]. García-Rivas GDJ, Guerrero-Hernández A, Guerrero-Serna G, Rodríguez-Zavala JS, Zazueta C, Inhibition of the mitochondrial calcium uniporter by the oxo-bridged dinuclear ruthenium amine complex (Ru360) prevents from irreversible injury in postischemic rat heart, FEBS Journal. 272 (2005) 3477–3488. 10.1111/j.1742-4658.2005.04771.x. [PubMed: 15978050]

[15]. Patron M, Raffaello A, Granatiero V, Tosatto A, Merli G, De Stefani D, Wright L, Pallafacchina G, Terrin A, Mammucari C, Rizzuto R, The mitochondrial calcium uniporter (MCU): molecular identity and physiological roles, J. Biol. Chem 288 (2013) 10750–10758. 10.1074/jbc.R112.420752. [PubMed: 23400777]

[16]. Liu JC, Parks RJ, Liu J, Stares J, Rovira II, Murphy E, Finkel T, The In Vivo Biology of the Mitochondrial Calcium Uniporter, Adv. Exp. Med. Biol 982 (2017) 49–63. 10.1007/978-3-319-55330-6_3. [PubMed: 28551781]

[17]. Baughman JM, Perocchi F, Girgis HS, Plovanich M, Belcher-Timme CA, Sancak Y, Bao XR, Strittmatter L, Goldberger O, Bogorad RL, Koteliansky V, Mootha VK, Integrative genomics identifies MCU as an essential component of the mitochondrial calcium uniporter, Nature. 476 (2011) 341–345. 10.1038/nature10234. [PubMed: 21685886]

[18]. De Stefani D, Raffaello A, Teardo E, Szabò I, Rizzuto R, A forty-kilodalton protein of the inner membrane is the mitochondrial calcium uniporter, Nature. 476 (2011) 336–340. 10.1038/nature10230. [PubMed: 21685888]

[19]. Raffaello A, De Stefani D, Sabbadin D, Teardo E, Merli G, Picard A, Checchetto V, Moro S, Szabò I, Rizzuto R, The mitochondrial calcium uniporter is a multimer that can include a dominant-negative pore-forming subunit, EMBO J 32 (2013) 2362–2376. 10.1038/emboj.2013.157. [PubMed: 23900286]

[20]. Mallilankaraman K, Doonan P, Cárdenas C, Chandramoorthy HC, Müller M, Miller R, Hoffman NE, Gandhirajan RK, Molgó J, Birnbaum MJ, Rothberg BS, Mak D-OD, Foskett JK, Madesh M, MICU1 is an essential gatekeeper for MCU-mediated mitochondrial Ca(2+) uptake that regulates cell survival, Cell. 151 (2012) 630–644. 10.1016/j.cell.2012.10.011. [PubMed: 23101630]

[21]. Plovanich M, Bogorad RL, Sancak Y, Kamer KJ, Strittmatter L, Li AA, Girgis HS, Kuchimanchi S, De Groot J, Speciner L, Taneja N, Oshea J, Koteliansky V, Mootha VK, MICU2, a paralog of MICU1, resides within the mitochondrial uniporter complex to regulate calcium handling, PLoS ONE. 8 (2013) e55785. 10.1371/journal.pone.0055785. [PubMed: 23409044]

[22]. Patron M, Granatiero V, Espino J, Rizzuto R, De Stefani D, MICU3 is a tissue-specific enhancer of mitochondrial calcium uptake, Cell Death & Differentiation. 26 (2019) 179–195. 10.1038/s41418-018-0113-8. [PubMed: 29725115]

[23]. Sancak Y, Markhard AL, Kitami T, Kovács-Bogdán E, Kamer KJ, Udeshi ND, Carr SA, Chaudhuri D, Clapham DE, Li AA, Calvo SE, Goldberger O, Mootha VK, EMRE is an essential component of the mitochondrial calcium uniporter complex, Science. 342 (2013) 1379–1382. 10.1126/science.1242993. [PubMed: 24231807]

[24]. Tsai M-F, Phillips CB, Ranaghan M, Tsai C-W, Wu Y, Willliams C, Miller C, Dual functions of a small regulatory subunit in the mitochondrial calcium uniporter complex, Elife. 5 (2016). 10.7554/eLife.15545.

[25]. Wang Y, Nguyen NX, She J, Zeng W, Yang Y, Bai X, Jiang Y, Structural Mechanism of EMRE-Dependent Gating of the Human Mitochondrial Calcium Uniporter, Cell. 177 (2019) 1252–1261.e13. 10.1016/j.cell.2019.03.050. [PubMed: 31080062]

[26]. Pan X, Liu J, Nguyen T, Liu C, Sun J, Teng Y, Fergusson MM, Rovira II, Allen M, Springer DA, Aponte AM, Gucek M, Balaban RS, Murphy E, Finkel T, The physiological role of mitochondrial calcium revealed by mice lacking the mitochondrial calcium uniporter, Nat. Cell Biol 15 (2013) 1464–1472. 10.1038/ncb2868. [PubMed: 24212091]

[27]. Pan X, Liu J, Nguyen T, Liu C, Sun J, Teng Y, Fergusson MM, Rovira II, Allen M, Springer DA, Aponte AM, Gucek M, Balaban RS, Murphy E, Finkel T, The physiological role of

mitochondrial calcium revealed by mice lacking the mitochondrial calcium uniporter, Nat. Cell Biol 15 (2013) 1464–1472. 10.1038/ncb2868. [PubMed: 24212091]

[28]. Holmström KM, Pan X, Liu JC, Menazza S, Liu J, Nguyen TT, Pan H, Parks RJ, Anderson S, Noguchi A, Springer D, Murphy E, Finkel T, Assessment of cardiac function in mice lacking the mitochondrial calcium uniporter, J. Mol. Cell. Cardiol 85 (2015) 178–182. 10.1016/j.yjmcc.2015.05.022. [PubMed: 26057074]

[29]. Rasmussen TP, Wu Y, Joiner MA, Koval OM, Wilson NR, Luczak ED, Wang Q, Chen B, Gao Z, Zhu Z, Wagner BA, Soto J, McCormick ML, Kutschke W, Weiss RM, Yu L, Boudreau RL, Abel ED, Zhan F, Spitz DR, Buettner GR, Song L-S, Zingman LV, Anderson ME, Inhibition of MCU forces extramitochondrial adaptations governing physiological and pathological stress responses in heart, Proc. Natl. Acad. Sci. U.S.A 112 (2015) 9129–9134. 10.1073/pnas.1504705112. [PubMed: 26153425]

[30]. Kwong JQ, Lu X, Correll RN, Schwanekamp JA, Vagnozzi RJ, Sargent MA, York AJ, Zhang J, Bers DM, Molkentin JD, The Mitochondrial Calcium Uniporter Selectively Matches Metabolic Output to Acute Contractile Stress in the Heart, Cell Rep. 12 (2015) 15–22. 10.1016/j.celrep.2015.06.002. [PubMed: 26119742]

[31]. Luongo TS, Lambert JP, Yuan A, Zhang X, Gross P, Song J, Shanmughapriya S, Gao E, Jain M, Houser SR, Koch WJ, Cheung JY, Madesh M, Elrod JW, The Mitochondrial Calcium Uniporter Matches Energetic Supply with Cardiac Workload during Stress and Modulates Permeability Transition, Cell Rep. 12 (2015) 23–34. 10.1016/j.celrep.2015.06.017. [PubMed: 26119731]

[32]. Liu JC, Syder NC, Ghorashi NS, Willingham TB, Parks RJ, Sun J, Fergusson MM, Liu J, Holmström KM, Menazza S, Springer DA, Liu C, Glancy B, Finkel T, Murphy E, EMRE is essential for mitochondrial calcium uniporter activity in a mouse model, JCI Insight. 5 (2020) 134063. 10.1172/jci.insight.134063. [PubMed: 32017711]

[33]. Chapoy-Villanueva H, Silva-Platas C, Gutiérrez-Rodríguez AK, García N, Acuña-Morin E, Elizondo-Montemayor L, Oropeza-Almazán Y, Aguilar-Saenz A, García-Rivas G, Changes in the Stoichiometry of Uniplex Decrease Mitochondrial Calcium Overload and Contribute to Tolerance of Cardiac Ischemia/Reperfusion Injury in Hypothyroidism, Thyroid. 29 (2019) 1755–1764. 10.1089/thy.2018.0668. [PubMed: 31456501]

[34]. Sverdlov AL, Elezaby A, Qin F, Behring JB, Luptak I, Calamaras TD, Siwik DA, Miller EJ, Liesa M, Shirihai OS, Pimentel DR, Cohen RA, Bachschmid MM, Colucci WS, Mitochondrial Reactive Oxygen Species Mediate Cardiac Structural, Functional, and Mitochondrial Consequences of Diet-Induced Metabolic Heart Disease, JAHA. 5 (2016). 10.1161/JAHA.115.002555.

[35]. Liu JC, Liu J, Holmström KM, Menazza S, Parks RJ, Fergusson MM, Yu Z-X, Springer DA, Halsey C, Liu C, Murphy E, Finkel T, MICU1 Serves as a Molecular Gatekeeper to Prevent In Vivo Mitochondrial Calcium Overload, Cell Rep. 16 (2016) 1561–1573. 10.1016/j.celrep.2016.07.011. [PubMed: 27477272]

[36]. Yang K, Doan MT, Stiles L, Divakaruni AS, Measuring CPT-1-mediated respiration in permeabilized cells and isolated mitochondria, STAR Protocols. 2 (2021) 100687. 10.1016/j.xpro.2021.100687. [PubMed: 34401773]

[37]. Spinazzi M, Casarin A, Pertegato V, Salviati L, Angelini C, Assessment of mitochondrial respiratory chain enzymatic activities on tissues and cultured cells, Nat Protoc. 7 (2012) 1235–1246. 10.1038/nprot.2012.058. [PubMed: 22653162]

[38]. Tsai C-W, Wu Y, Pao P-C, Phillips CB, Williams C, Miller C, Ranaghan M, Tsai M-F, Proteolytic control of the mitochondrial calcium uniporter complex, Proc. Natl. Acad. Sci. U.S.A 114 (2017) 4388–4393. 10.1073/pnas.1702938114. [PubMed: 28396416]

[39]. Glancy B, Balaban RS, Role of mitochondrial Ca2+ in the regulation of cellular energetics, Biochemistry. 51 (2012) 2959–2973. 10.1021/bi2018909. [PubMed: 22443365]

[40]. Altamimi TR, Karwi QG, Uddin GM, Fukushima A, Kwong JQ, Molkentin JD, Lopaschuk GD, Cardiac-specific deficiency of the mitochondrial calcium uniporter augments fatty acid oxidation and functional reserve, J. Mol. Cell. Cardiol 127 (2019) 223–231. 10.1016/j.yjmcc.2018.12.019. [PubMed: 30615880]

[41]. Gherardi G, Nogara L, Ciciliot S, Fadini GP, Blaauw B, Braghetta P, Bonaldo P, De Stefani D, Rizzuto R, Mammucari C, Loss of mitochondrial calcium uniporter rewires skeletal

muscle metabolism and substrate preference, Cell Death Differ. 26 (2019) 362–381. 10.1038/s41418-018-0191-7. [PubMed: 30232375]

[42]. Kwong JQ, Huo J, Bround MJ, Boyer JG, Schwanekamp JA, Ghazal N, Maxwell JT, Jang YC, Khuchua Z, Shi K, Bers DM, Davis J, Molkentin JD, The mitochondrial calcium uniporter underlies metabolic fuel preference in skeletal muscle, JCI Insight. 3 (2018). 10.1172/jci.insight.121689.

[43]. Sommakia S, Houlihan PR, Deane SS, Simcox JA, Torres NS, Jeong M-Y, Winge DR, Villanueva CJ, Chaudhuri D, Mitochondrial cardiomyopathies feature increased uptake and diminished efflux of mitochondrial calcium, J Mol Cell Cardiol. 113 (2017) 22–32. 10.1016/j.yjmcc.2017.09.009. [PubMed: 28962857]

[44]. Balderas E, Eberhardt DR, Lee S, Pleinis JM, Sommakia S, Balynas AM, Yin X, Parker MC, Maguire CT, Cho S, Szulik MW, Bakhtina A, Bia RD, Friederich MW, Locke TM, Van Hove JLK, Drakos SG, Sancak Y, Tristani-Firouzi M, Franklin S, Rodan AR, Chaudhuri D, Mitochondrial calcium uniporter stabilization preserves energetic homeostasis during Complex I impairment, Nat Commun. 13 (2022) 2769. 10.1038/s41467-022-30236-4. [PubMed: 35589699]

[45]. Wang P, Xu S, Xu J, Xin Y, Lu Y, Zhang H, Zhou B, Xu H, Sheu S-S, Tian R, Wang W, Elevated MCU Expression by CaMKIIδB Limits Pathological Cardiac Remodeling, Circulation. 145 (2022) 1067–1083. 10.1161/CIRCULATIONAHA.121.055841. [PubMed: 35167328]

[46]. Koval OM, Nguyen EK, Santhana V, Fidler TP, Sebag SC, Rasmussen TP, Mittauer DJ, Strack S, Goswami PC, Abel ED, Grumbach IM, Loss of MCU prevents mitochondrial fusion in G1-S phase and blocks cell cycle progression and proliferation, Sci Signal. 12 (2019). 10.1126/scisignal.aav1439.

[47]. Bernardi P, Rasola A, Forte M, Lippe G, The Mitochondrial Permeability Transition Pore: Channel Formation by F-ATP Synthase, Integration in Signal Transduction, and Role in Pathophysiology, Physiological Reviews. 95 (2015) 1111–1155. 10.1152/physrev.00001.2015. [PubMed: 26269524]

[48]. Kosmach A, Roman B, Sun J, Femnou A, Zhang F, Liu C, Combs CA, Balaban RS, Murphy E, Monitoring mitochondrial calcium and metabolism in the beating MCU-KO heart, Cell Reports. 37 (2021) 109846. 10.1016/j.celrep.2021.109846. [PubMed: 34686324]

[49]. Davis J, Maillet M, Miano JM, Molkentin JD, Lost in transgenesis: a user's guide for genetically manipulating the mouse in cardiac research, Circ. Res 111 (2012) 761–777. 10.1161/CIRCRESAHA.111.262717. [PubMed: 22935533]

[50]. Connern CP, Halestrap AP, Recruitment of mitochondrial cyclophilin to the mitochondrial inner membrane under conditions of oxidative stress that enhance the opening of a calcium-sensitive non-specific channel, Biochem J 302 (Pt 2) (1994) 321–324. 10.1042/bj3020321. [PubMed: 7522435]

[51]. Parks RJ, Menazza S, Holmström KM, Amanakis G, Fergusson M, Ma H, Aponte AM, Bernardi P, Finkel T, Murphy E, Cyclophilin D-mediated regulation of the permeability transition pore is altered in mice lacking the mitochondrial calcium uniporter, Cardiovascular Research. 115 (2019) 385–394. 10.1093/cvr/cvy218. [PubMed: 30165576]

Highlights

- A tamoxifen-inducible, cardiac-specific mouse model of *Emre* deletion was generated
- Mitochondrial Ca^{2+} uptake is eliminated after short and long-term EMRE loss
- Response to adrenergic stimulation is blunted after short and long-term EMRE loss
- Short-term EMRE loss is protective against ischemia/reperfusion (I/R) injury
- Protection against I/R injury is lost in the long-term absence of EMRE

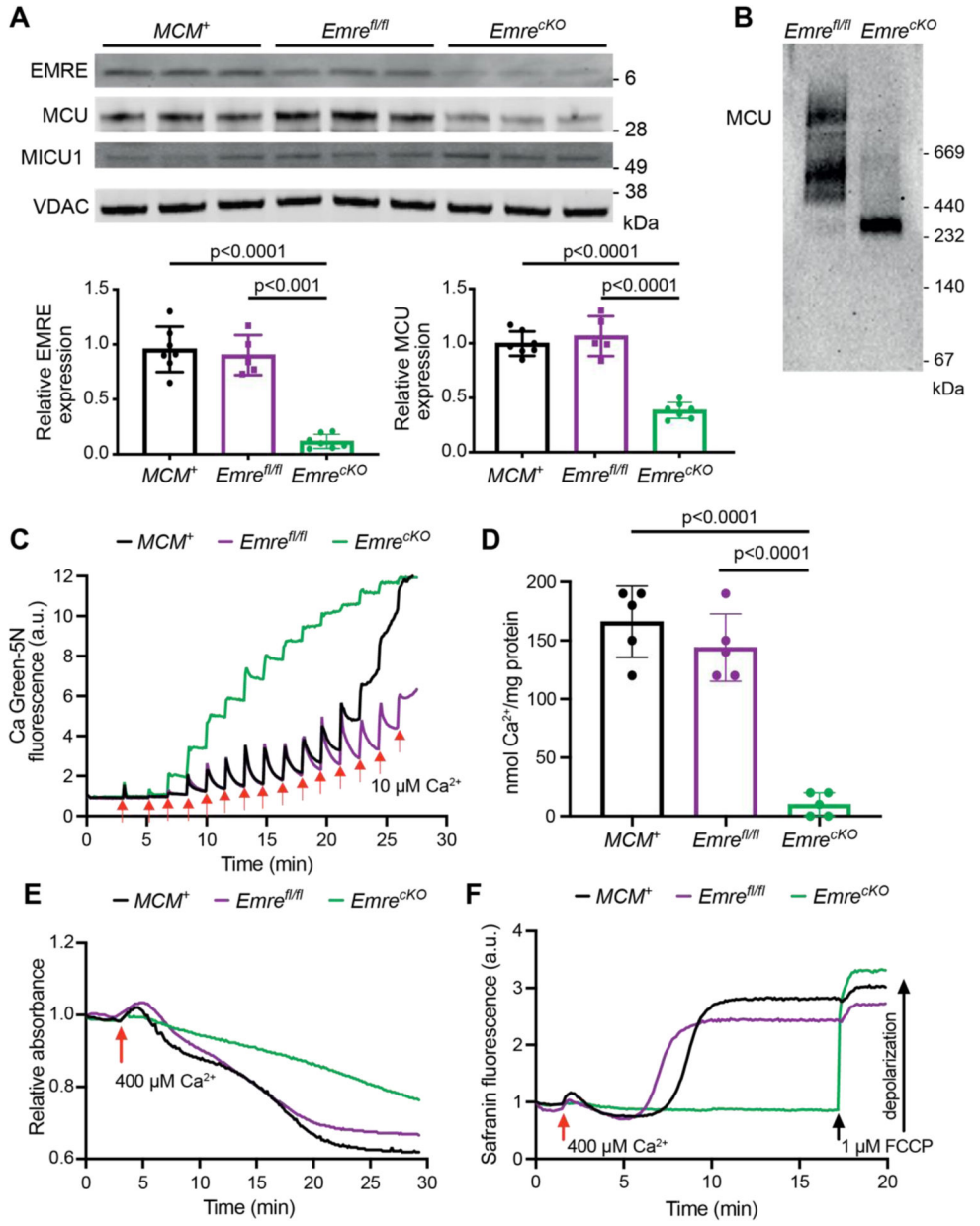

Figure 1. Short-term Emre deletion impairs mitochondrial Ca^{2+} uptake.

Analyses were performed 3 weeks post-tamoxifen. **A**) Representative Western blot of EMRE, MCU, and MICU1 in cardiac mitochondria from *MCM*$^{+}$, *Emre*$^{fl/fl}$ and *Emre*^{cKO} mice. VDAC was used as a loading control. Below, Western blot quantification shows a 90% reduction in EMRE and a 60% reduction in MCU in *Emre*^{cKO} mitochondria compared to control groups. Values represent mean ± SD.**p<0.0001, n = 7 in *MCM*$^{+}$ and *Emre*^{cKO}, n = 5 in *Emre*$^{fl/fl}$. One-way ANOVA test was used for statistical analysis. **B**) Blue Native gel of freshly isolated mitochondria from *Emre*$^{fl/fl}$ and *Emre*^{cKO} hearts, immunoblotted with MCU antibody. Gel is representative of 3 mice (combined males and females) per group. **C**) Representative Ca^{2+} retention capacity (CRC) assay in isolated heart mitochondria from *MCM*$^{+}$ (black line), *Emre*$^{fl/fl}$ (purple line) and *Emre*^{cKO} (green line) mice. The

fluorescent Ca^{2+} indicator Calcium Green-5N was used to monitor extramitochondrial Ca^{2+}. The arrows represent 10 μM Ca^{2+} additions. Traces are representative of n = 5 independent experiments. **D**) Ca^{2+} retention capacity calculated from independent traces as shown in (C). The estimated mean Ca^{2+}/mg protein was for MCM^{+}: 166 ± 30.49, for $Emre^{fl/fl}$: 144 ± 28.89, and for $Emre^{cKO}$: 10 ± 5 nmol of Ca^{2+}/mg protein. Values represent mean ± SD.**p<0.0001, n = 5 per group. One-way ANOVA test was used for statistical analysis. **E**) Representative mitochondrial swelling assay monitoring absorbance of isolated heart mitochondria from MCM^{+} (black line), $Emre^{fl/fl}$ (purple line) and $Emre^{cKO}$ (green line) mice after addition of 400 μM Ca^{2+}. Traces are representative of n = 5 independent experiments. **F**) Representative traces of safranin fluorescence as an indicator of membrane potential ($\Delta\Psi$) depolarization in isolated heart mitochondria from MCM^{+} (black line), $Emre^{fl/fl}$ (purple line) and $Emre^{cKO}$ (green line) mice after addition of 400 μM Ca^{2+}. As a positive control in $Emre^{cKO}$ mitochondria, depolarization was induced by addition of 1 μM FCCP. Traces are representative of n = 4 independent experiments. The mean time to Ca^{2+}-induced depolarization, calculated as the time from Ca^{2+} addition to 50% of the rise in fluorescence, was for MCM^{+}: 9.1 ± 2.8 minutes, for $Emre^{fl/fl}$: 5.9 ± 1 minute, and could not be calculated for $Emre^{cKO}$ as FCCP was required for depolarization.

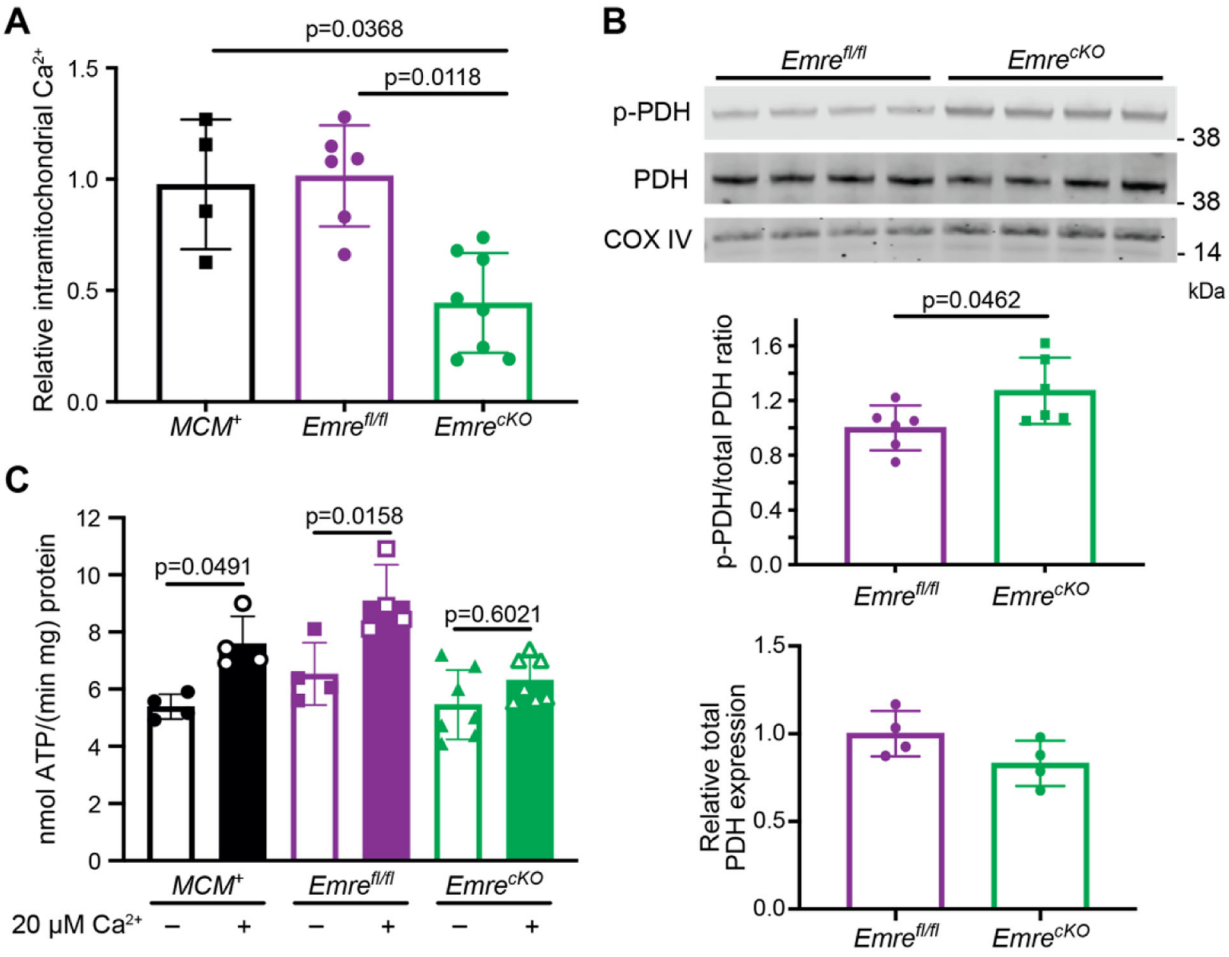

Figure 2. Short-term Emre deletion leads to lower intramitochondrial Ca^{2+} content and attenuated Ca^{2+}-stimulated ATP production.

Analyses were performed 3 weeks post-tamoxifen. **A**) Quantification of relative free $_{m}Ca^{2+}$. *Emre*^{cKO} mitochondria show a reduction in $_{m}Ca^{2+}$ by 56% relative to controls. n=4–8, *p<0.05. One-way ANOVA was used for statistical analysis. **B**) Representative Western blot of phosphorylated PDH (p-PDH) and total PDH from *Emre*$^{fl/fl}$ and *Emre*^{cKO} mitochondria. COX IV was used as a loading control. Below, Western blot quantification shows a 25% increase in p-PDH to total PDH ratio in *Emre*^{cKO} relative to *Emre*$^{fl/fl}$ mitochondria. n=6 per group. Student *t*-test was used for statistical analysis. **C**) Analysis of ATP production rate in isolated heart mitochondria stimulated with 50 μM ADP and 10 mM succinate ± 20 μM Ca^{2+}. *MCM*$^{+}$: 5.39 ± 0.43 *vs MCM*$^{+}$ + 20 μM Ca^{2+}: 7.59 ± 0.96, *Emre*$^{fl/fl}$: 6.35 ± 1.09 *vs Emre*$^{fl/fl}$ + 20 μM Ca^{2+}: 9.01 ± 1.25, and *Emre*^{cKO}: 5.46 ± 1.21 *vs Emre*^{cKO} + 20 μM Ca^{2+}: 6.32 ± 0.78 nmol ATP/(min*mg) protein. Values represent mean ± SD. *p<0.05, n=4–7. One-way ANOVA was used for statistical analysis.

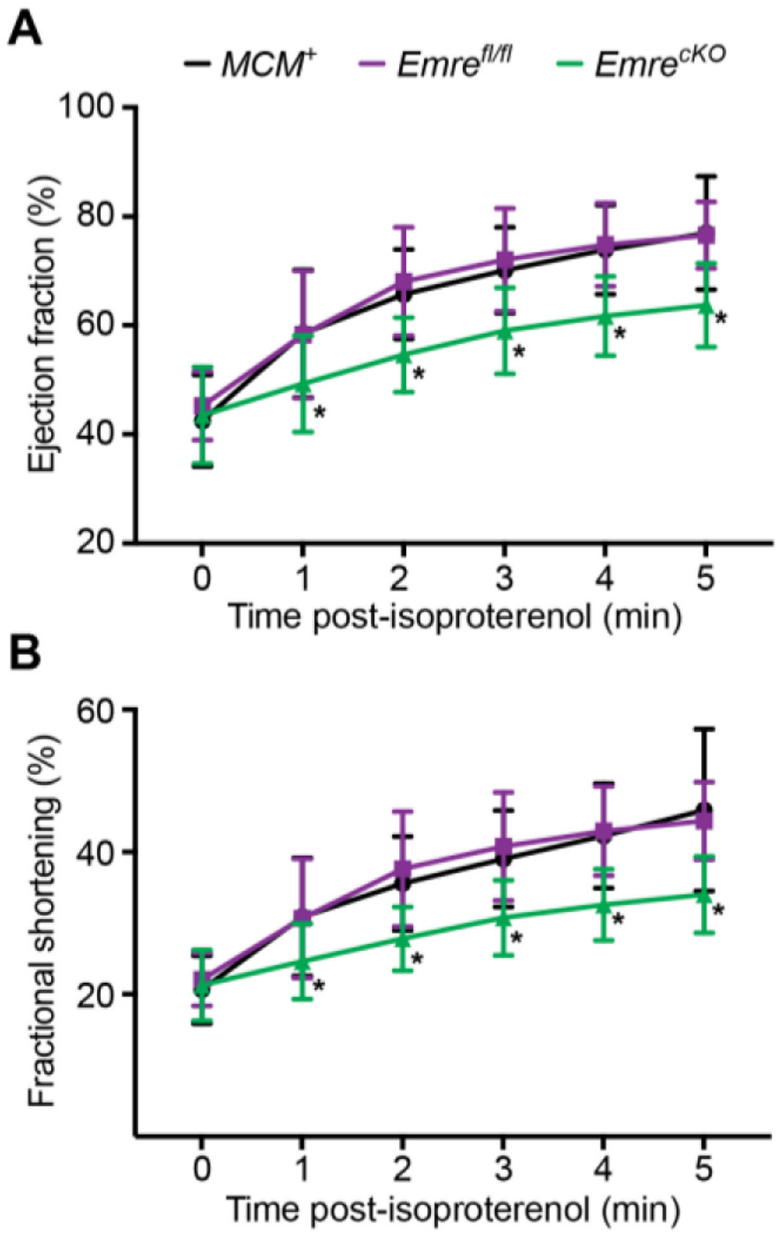

Figure 3. Short-term Emre deletion leads to reduced response to β-adrenergic stimulation.

Three weeks post-tamoxifen, echocardiography at baseline (time 0), then 1, 2, 3, 4 and 5 minutes after isoproterenol injection (0.4 μg/kg) was used to analyze **A**) ejection fraction (EF) and **B**) fractional shortening (FS). A) EF at minute 5: MCM^{+}: 76.95% ± 10.38, $Emre^{fl/fl}$: 76.55% ± 6.11 and $Emre^{cKO}$: 63.70% ± 7.65. B) FS at minute 5: MCM^{+}: 45.90% ± 11.39, $Emre^{fl/fl}$: 44.38% ± 5.45 and $Emre^{cKO}$: 34.01% ± 5.38. Values represent mean ± SD. *p<0.05, n=14–16 per group. Two-way ANOVA test was used for statistical analysis.

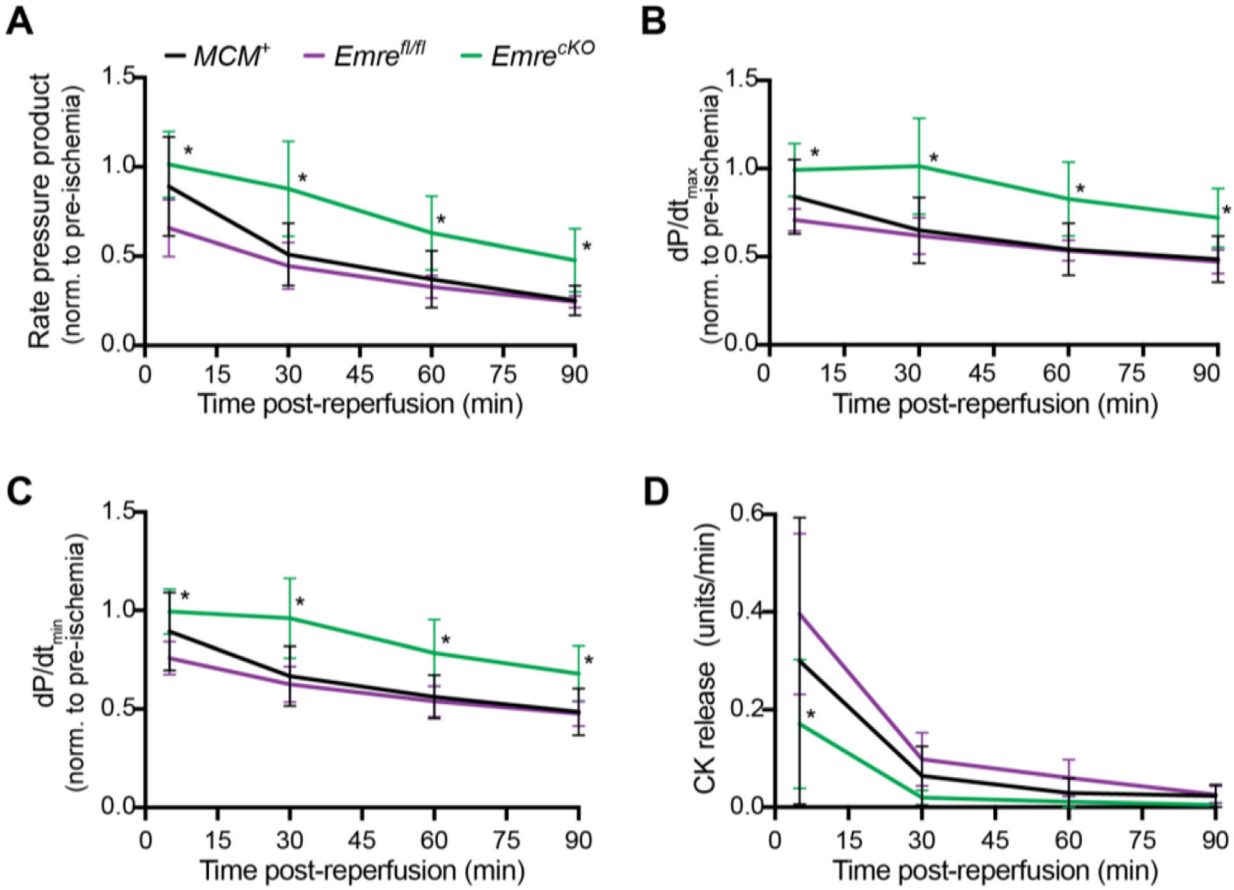

Figure 4. Short-term Emre deletion preserves cardiac function in I/R.

Three weeks post-tamoxifen, mouse hearts were subjected to 20 minutes of stabilization, 20 minutes of global ischemia and 90 minutes of reperfusion. At 5, 30, 60, and 90 minutes after the onset of reperfusion, relative to baseline pre-ischemia, **A**) rate pressure product (RPP) = heart rate (HR) × left ventricular pressure (LVP), **B**) dP/dt_{max}, **C**) dP/dt_{min}, and **D**) creatine kinase (CK) release were assessed. Values at 90 minutes: A) RPP: MCM^{+}: 50.96% ± 17.39, $Emre^{fl/fl}$: 44.55% ± 13.05 and $Emre^{cKO}$: 87.64% ± 26.68. B) dP/dt_{max}: MCM^{+}: 48.50% ± 13.10, $Emre^{fl/fl}$: 47.14% ± 6.74 and $Emre^{cKO}$: 72.04% ± 16.62. C) dP/dt_{min}: MCM^{+}: 48.53% ± 11.95, $Emre^{fl/fl}$: 47.64% ± 6.45 and $Emre^{cKO}$: 67.88% ± 14.23. Values represent mean ± SD. *p<0.05, n=5–6 per group. Two-way ANOVA test was used for statistical analysis.

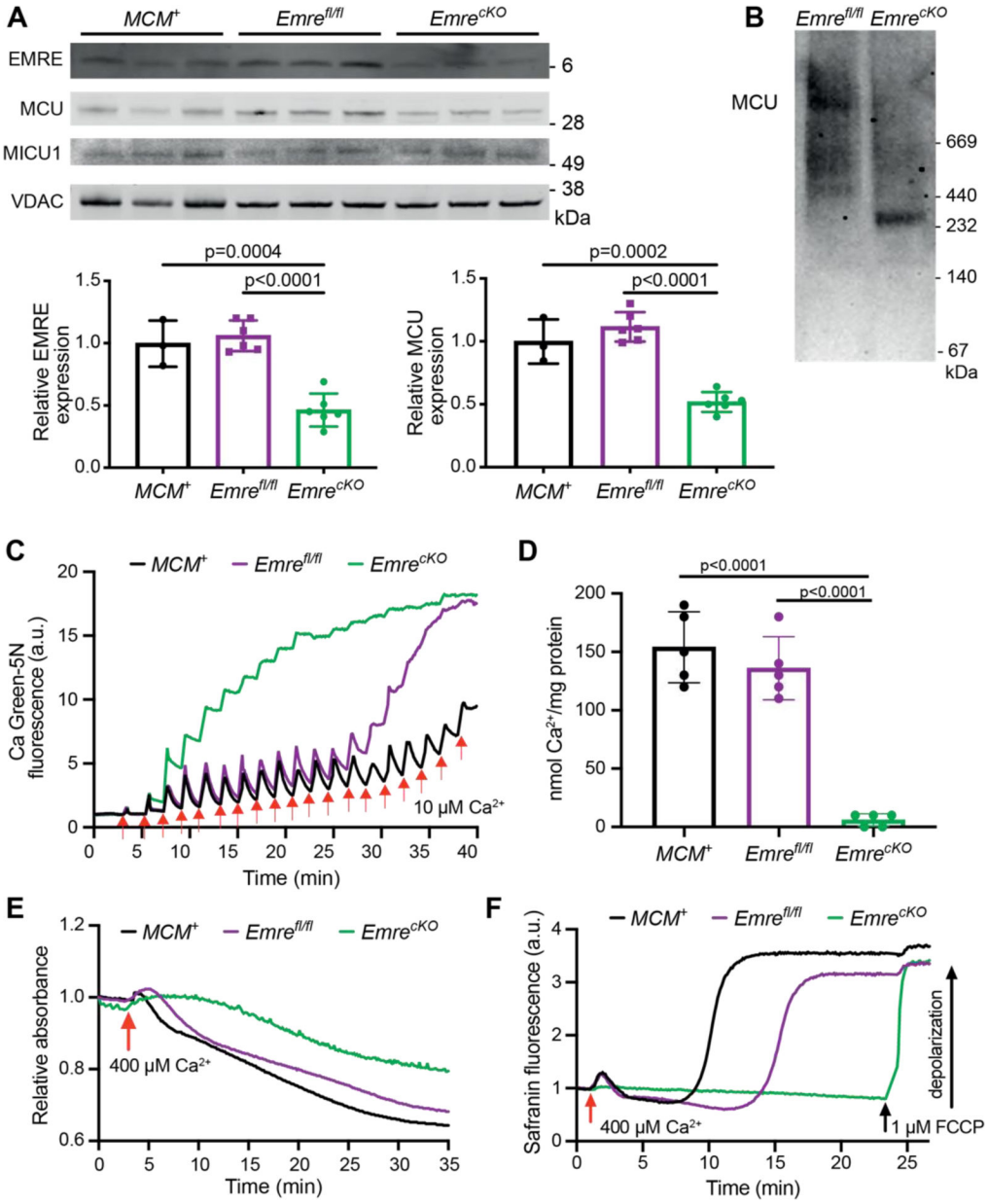

Figure 5. Mitochondrial Ca^{2+} handling remains impaired with long-term Emre deletion.

Analyses were performed 3 months post-tamoxifen. **A**) Representative Western blot of EMRE, MCU, and MICU1 in cardiac mitochondria from *MCM*$^{+}$, *Emre*$^{fl/fl}$ and *Emre*^{cKO} mice. VDAC was used as a loading control. Below, Western blot quantification of mitochondria from *MCM*$^{+}$ (n = 3), *Emre*$^{fl/fl}$ (n = 6), and *Emre*^{cKO} (n = 6) hearts. Values represent mean ± SD. One-way ANOVA was used for statistical analysis. **B**) Blue Native gel of freshly isolated mitochondria from *Emre*$^{fl/fl}$ and *Emre*^{cKO} hearts, immunoblotted with MCU antibody. Gel is representative of 3 mice (combined males and females) per group. **C**) Representative Ca^{2+} retention capacity (CRC) assay in isolated heart mitochondria from *MCM*$^{+}$ (black line), *Emre*$^{fl/fl}$ (purple line) and *Emre*^{cKO} (green line) mice. The fluorescent Ca^{2+} indicator Calcium Green-5N was used to monitor extramitochondrial Ca^{2+}. The arrows

represent 10 μM Ca^{2+} added. Traces are representative of n = 5 independent experiments. **D**) Ca^{2+} retention capacity calculated from independent traces as shown in (C). The estimated mean Ca^{2+}/mg protein was for MCM^{+} : 154 ± 30.50, $Emre^{fl/fl}$: 136 ± 27.01 and $Emre^{cKO}$: 6 ± 5.47 nmol of Ca^{2+} / mg protein. Values represent mean ± SD.**p<0.0001, n = 5 in each group. One-way ANOVA test was used for statistical analysis. **E**) Representative mitochondrial swelling assay monitoring absorbance of isolated heart mitochondria from MCM^{+} (black line), $Emre^{fl/fl}$ (purple line) and $Emre^{cKO}$ (green line) mice after addition of 400 μM Ca^{2+}. Traces are representative of n = 5 independent experiments. **F**) Representative traces of membrane potential (ΔΨ) depolarization in isolated heart mitochondria from MCM^{+} (black line), $Emre^{fl/fl}$ (purple line) and $Emre^{cKO}$ (green line) mice after the addition of 400 μM Ca^{2+}. As a positive control in $Emre^{cKO}$ mitochondria, depolarization was induced by addition of 1 μM FCCP. Traces are representative of n = 4 independent experiments. The mean time to Ca^{2+}-induced depolarization, calculated as the time from Ca^{2+} addition to 50% of the rise in fluorescence, was for MCM^{+}: 10.5 ± 2 minutes, for $Emre^{fl/fl}$: 12.7 ± 2.3 minutes, and could not be calculated for $Emre^{cKO}$ as FCCP was required for depolarization.

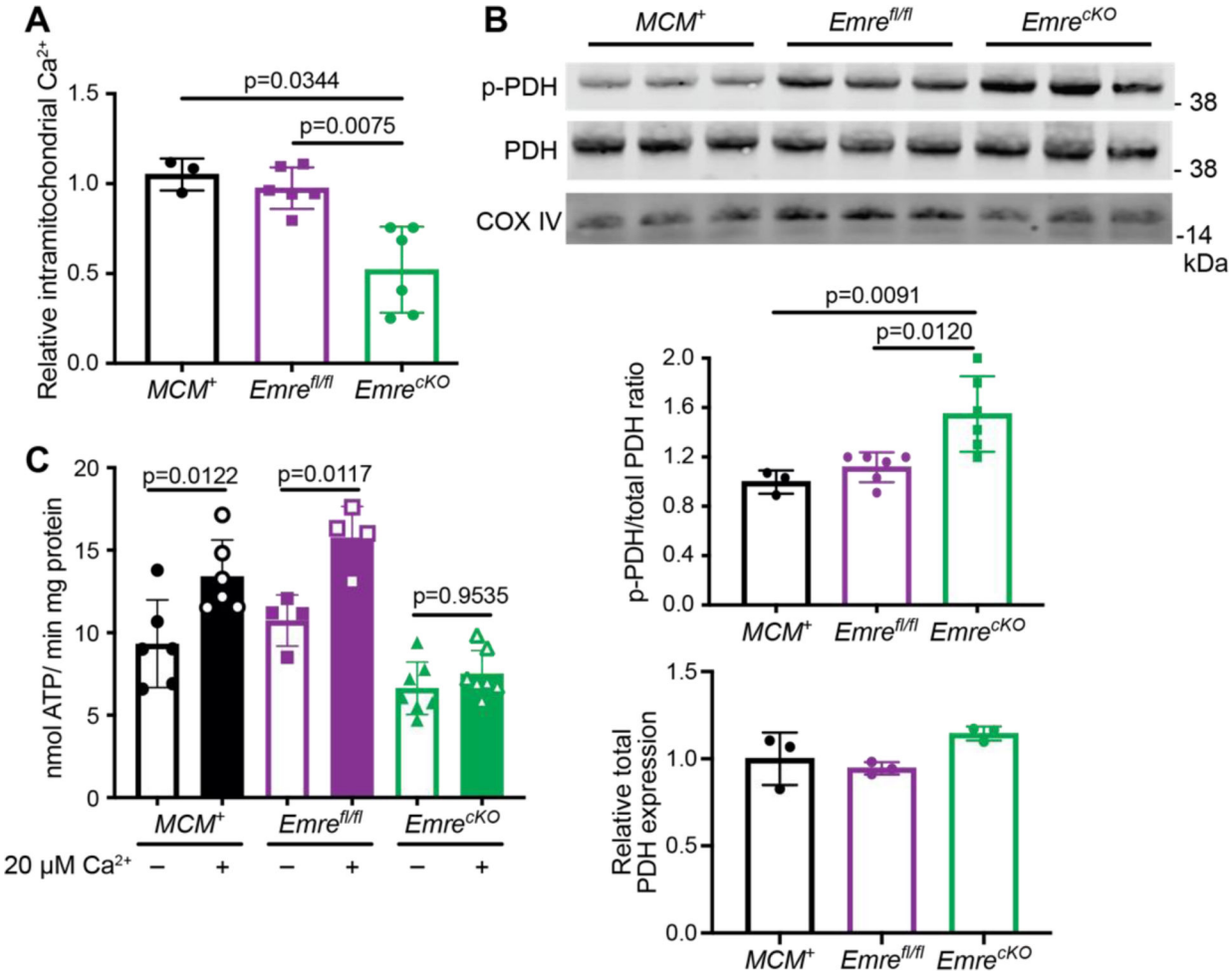

Figure 6. Lower intramitochondrial Ca^{2+} content and attenuated Ca^{2+}-stimulated ATP production are maintained over long-term Emre deletion.

Analyses were performed 3 months post-tamoxifen. **A**) Quantification of relative free $_{m}Ca^{2+}$ in mitochondria from *MCM*$^{+}$ (n = 3), *Emre*$^{fl/fl}$ (n = 6), and *Emre*^{cKO} (n = 6) hearts. *Emre*^{cKO} mitochondria show a reduction in $_{m}Ca^{2+}$ by 40% ± 15.01 relative to controls. Values represent mean ± SD. One-way ANOVA was used for statistical analysis. **B**) Representative Western blot of phosphorylated PDH (p-PDH) and total PDH from *Emre*$^{fl/fl}$ and *Emre*^{cKO} mitochondria. COX IV was used as a loading control. Below, Western blot quantification of mitochondria from *MCM*$^{+}$ (n = 3), *Emre*$^{fl/fl}$ (n = 6), and *Emre*^{cKO} (n = 6) hearts. Values represent mean ± SD. One-way ANOVA was used for statistical analysis. **C**) ATP production rate in isolated heart mitochondria stimulated with 50 µM ADP and 10 mM succinate ± 20 µM Ca^{2+}. *MCM*$^{+}$: 9.33 ± 2.65 *vs MCM*$^{+}$+ 20 µM Ca^{2+}: 13.41 ± 2.21, *Emre*$^{fl/fl}$: 10.73 ± 1.55 *vs Emre*$^{fl/fl}$ + 20 µM Ca^{2+}: 15.76 ± 1.90, and *Emre*^{cKO}: 6.63 ± 1.59 *vs Emre*^{cKO} + 20 µM Ca^{2+}: 7.52 ± 1.40 nmol ATP/min*mg protein. Values represent mean ± SD. *p<0.05, n=4–7. One-way ANOVA was used for statistical analysis.

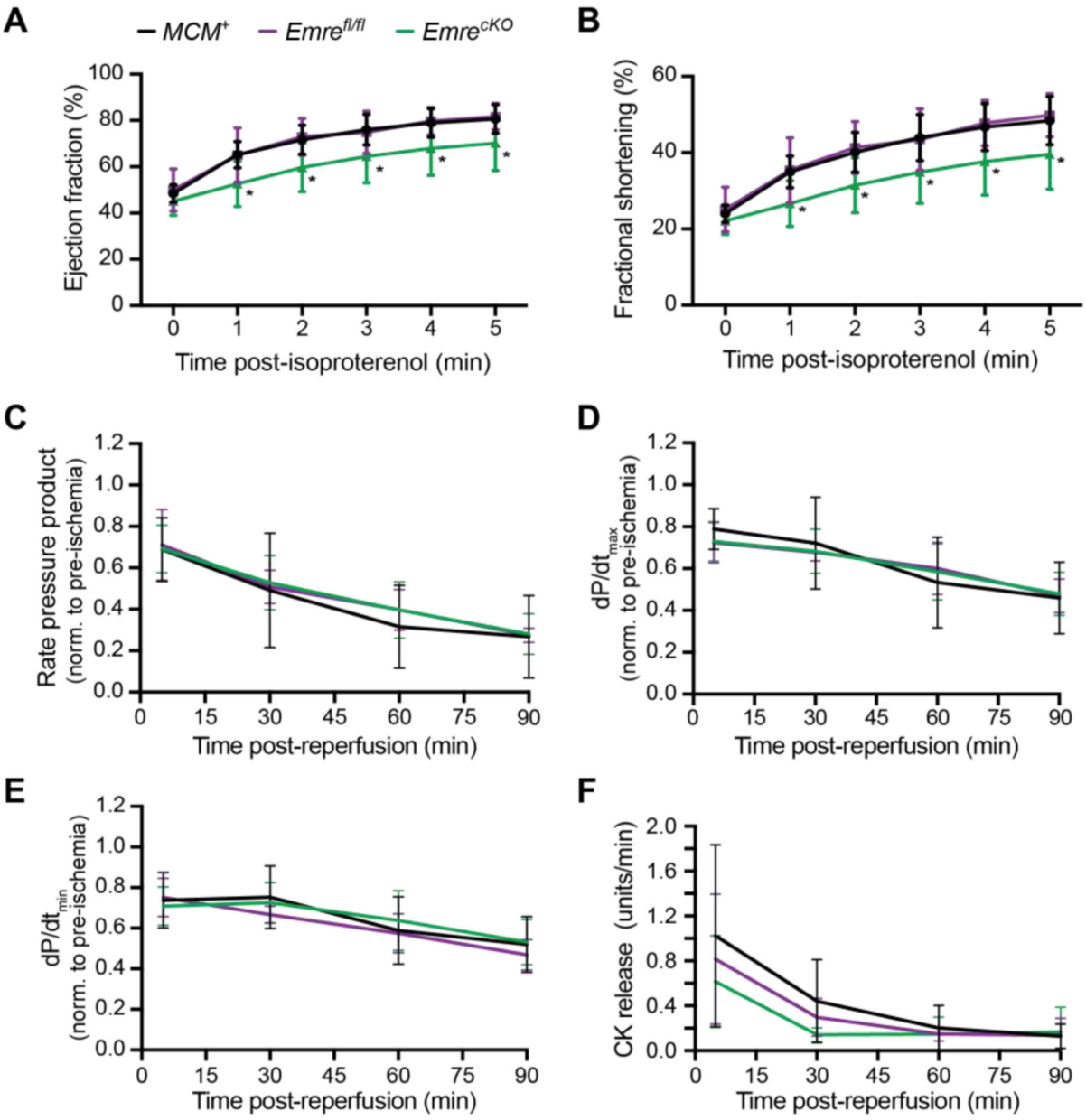

Figure 7. β-adrenergic response remains diminished in long-term Emre deletion, but protection against I/R injury is lost.

Three months post-tamoxifen, echocardiography at baseline (time 0), then 1, 2, 3, 4 and 5 minutes after isoproterenol injection (0.4 μg/kg) was used to analyze **A**) ejection fraction (EF) and **B**) fractional shortening (FS). A) EF at minute 5: *MCM*$^{+}$(black line): 80.58% ± 6.19, *Emre*$^{fl/fl}$ (purple line): 81.62% ± 5.69 and *Emre*^{cKO} (green line): 70.20% ± 11.08. B) FS at minute 5: *MCM*$^{+}$: 48.42% ± 6.32, *Emre*$^{fl/fl}$: 49.80% ± 5.67 and *Emre*^{cKO}: 39.58% ± 9.14. Values represent mean ± SD. *p<0.05, n=10–12 per group. Two-way ANOVA was used for statistical analysis. Three months post-tamoxifen, mouse hearts were subjected to 20 minutes of stabilization, 20 minutes of global ischemia and 90 minutes of reperfusion. At 5, 30, 60, and 90 minutes after the onset of reperfusion, relative to baseline pre-ischemia, **C**) rate pressure product (RPP) = heart rate (HR) × left ventricular pressure (LVP), **D**) dP/dt_{max},

E) dP/dt_{min}, and **F**) creatine kinase (CK) release were assessed. Values represent mean ± SD. *$p<0.05$, n=5–6 per group. Two-way ANOVA was used for statistical analysis.

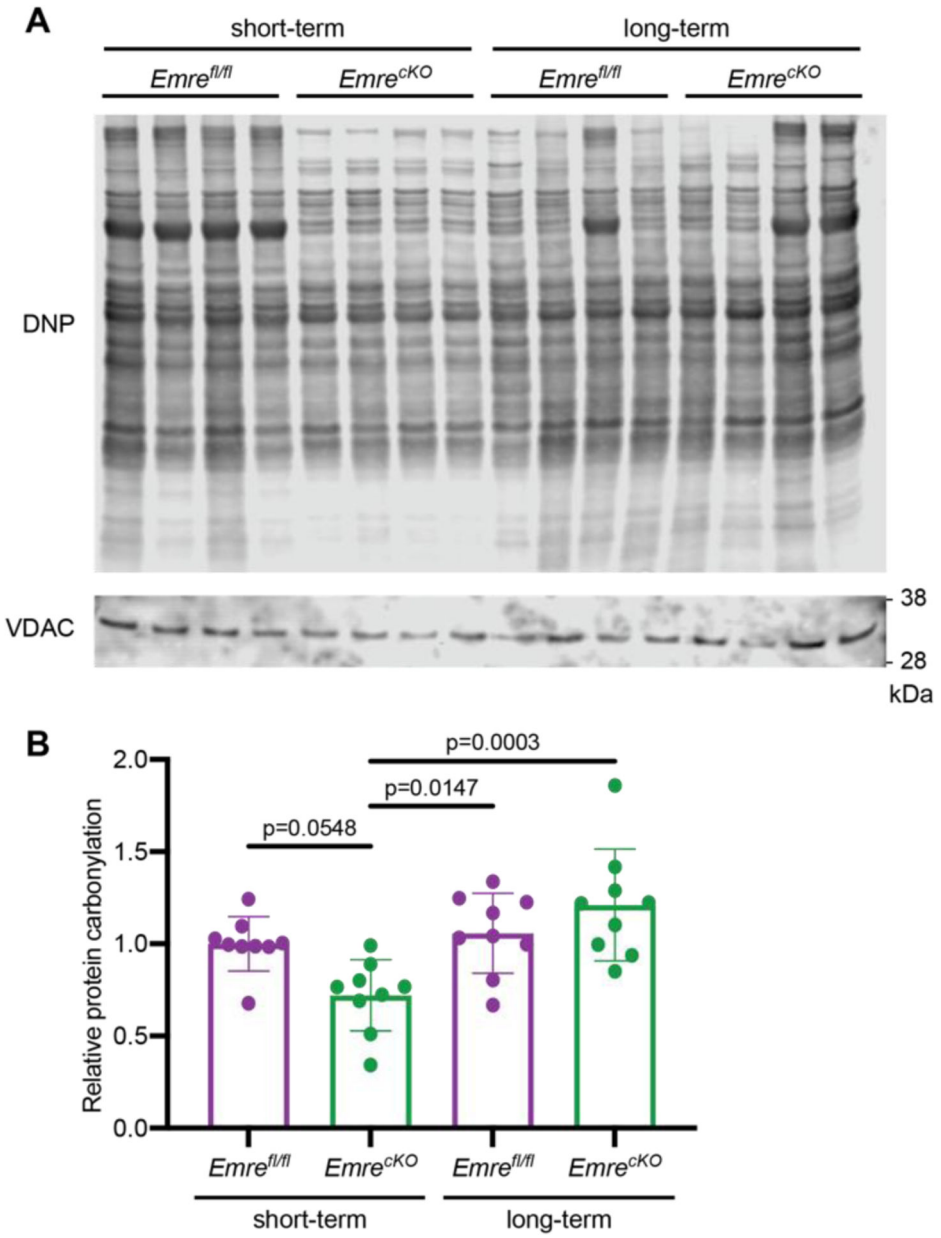

Figure 8. Short-term Emre deletion leads to lower oxidative stress levels than long-term Emre deletion.

A) Representative Western blot using anti-DNP antibody to detect carbonyl groups modified by DNPH as a marker of oxidized proteins in cardiac mitochondria from short-term and long-term *Emre*$^{fl/fl}$ and *Emre*^{cKO} mice. VDAC was used as a loading control. **B**) Western blot quantification of mitochondria from short-term *Emre*$^{fl/fl}$: 1.00 ± 0.14 (n = 9), short-term *Emre*^{cKO}: 0.72 ± 0.19 (n = 9), long-term *Emre*$^{fl/fl}$: 1.05 ± 0.21 (n = 9), and long-term *Emre*^{cKO}: 1.21 ± 0.30 (n = 9). Values represent mean ± SD, *p<0.05. One-way ANOVA was used for statistical analysis.

Table 1.

Genetic mouse models of mitochondrial Ca^{2+} uniporter inactivation.

Author and year	Knock out model	Tamoxifen route and dose	Timing of experiments	Response to β-adrenergic stimulation	Protection after ischemia/ reperfusion
Pan *et al,* 2013 [27]	global MCU deletion	N/A	age 3–5 months	unchanged	not protected, *ex vivo*
Rasmussen *et al,* 2015 [29]	cardiac (αMHC) expression of a dominant-negative MCU	N/A	unspecified	diminished	not protected, *ex vivo*
Kwong *et al,* 2015 [30]	cardiac (αMHC-MerCreMer) MCU deletion	chow 4 weeks	6 weeks post-tamoxifen	diminished	protected, *in vivo*
Luongo *et al,* 2015 [31]	cardiac (αMHC-MerCreMer) MCU deletion	injection, 40 mg/kg/day 5 days	10 days post-tamoxifen (hemodynamics) 3 weeks post-tamoxifen (IR)	diminished	protected, *in vivo*
Liu *et al,* 2020 [32]	global EMRE deletion	N/A	age 3–6 months	unchanged	not protected, *ex vivo*